2009

N-terminal inactivation domains of β subunits are protected from trypsin digestion by binding within the antechamber of BK channels

Zhe Zhang
Washington University School of Medicine in St. Louis
Xu-Hui Zeng
Washington University School of Medicine in St. Louis
Xiao-Ming Xia
Washington University School of Medicine in St. Louis
Christopher J. Lingle
Washington University School of Medicine in St. Louis

Published February 23, 2009

N-terminal Inactivation Domains of β Subunits Are Protected from Trypsin Digestion by Binding within the Antechamber of BK Channels

Zhe Zhang, Xu-Hui Zeng, Xiao-Ming Xia, and Christopher J. Lingle

Department of Anesthesiology, Washington University School of Medicine, St. Louis, MO 63110

N termini of auxiliary β subunits that produce inactivation of large-conductance Ca^{2+}-activated K^+ (BK) channels reach their pore-blocking position by first passing through side portals into an antechamber separating the BK pore module and the large C-terminal cytosolic domain. Previous work indicated that the β2 subunit inactivation domain is protected from digestion by trypsin when bound in the inactivated conformation. Other results suggest that, even when channels are closed, an inactivation domain can also be protected from digestion by trypsin when bound within the antechamber. Here, we provide additional tests of this model and examine its applicability to other β subunit N termini. First, we show that specific mutations in the β2 inactivation segment can speed up digestion by trypsin under closed-channel conditions, supporting the idea that the β2 N terminus is protected by binding within the antechamber. Second, we show that cytosolic channel blockers distinguish between protection mediated by inactivation and protection under closed-channel conditions, implicating two distinct sites of protection. Together, these results confirm the idea that β2 N termini can occupy the BK channel antechamber by interaction at some site distinct from the BK central cavity. In contrast, the β3a N terminus is digested over 10-fold more quickly than the β2 N terminus. Analysis of factors that contribute to differences in digestion rates suggests that binding of an N terminus within the antechamber constrains the trypsin accessibility of digestible basic residues, even when such residues are positioned outside the antechamber. Our analysis indicates that up to two N termini may simultaneously be protected from digestion. These results indicate that inactivation domains have sites of binding in addition to those directly involved in inactivation.

INTRODUCTION

Rapid inactivation of large-conductance Ca^{2+}-activated K^+ (BK) channels is mediated by N-terminal cytosolic hydrophobic peptide segments of auxiliary β subunits (Wallner et al., 1999; Xia et al., 1999; Uebele et al., 2000; Xia et al., 2000, 2003). Such peptide segments are thought to obstruct ion flux by binding within the BK channel central cavity. To access this binding site, β subunit N termini must approach the axis of the permeation pathway laterally (Fig. 1 A), passing through the so-called side portals (Gulbis et al., 2000; Kobertz et al., 2000) that separate the membrane-embedded pore module and the large cytosolic structure involved in ligand recognition (Zhang et al., 2006). BK β subunit N termini contain basic residues that can be attacked by trypsin, thereby removing β subunit–mediated inactivation. Using quantitative measurement of trypsin-mediated removal of inactivation, it has been shown that the space between the pore domain and cytosolic domain defines a volume in which the β2 N terminus is protected from digestion by trypsin, and this protected volume has been termed an antechamber (Zhang et al., 2006). The properties of removal by trypsin of β2-mediated inactivation are consistent with a model in which, even under conditions in which channels are closed, individual N termini occupy the antechamber for an appreciable fraction of time, thereby conferring some protection against digestion by trypsin (Fig. 1 B). Thus, a determinant of the time course of digestion by trypsin reflects not just the accessibility of the basic residues, but also the fraction of time a β2 N terminus resides within the protected antechamber.

The primary evidence supporting the protected antechamber idea arose from the observation that, under conditions that favor inactivation, digestion of the β2 N terminus was markedly slowed. The critical motif necessary for β2 subunit–mediated inactivation is a triplet of hydrophobic residues, FIW, that immediately follows the N-terminal methionine (Xia et al., 2003). Therefore, the trypsin susceptibility of a series of artificial N termini was examined for which basic residues were positioned at different distances from the FIW triplet. These experiments revealed that, when in an inactivated position, basic residues were protected from digestion only when they were positioned within 12 residues of the N-terminal FIW (Zhang et al., 2006). Interestingly,

Correspondence to Christopher J. Lingle: clingle@morpheus.wustl.edu

Abbreviations used in this paper: bbTBA, *N*-(4-[benzoyl]benzyl)-*N*,N,*N*-tributylammonium bromide; BK, large-conductance Ca^{2+}-activated K^+; TBA, tetrabutylammonium; TM1, transmembrane segment 1.

The Rockefeller University Press $30.00
J. Gen. Physiol. Vol. 133 No. 3 263–282
www.jgp.org/cgi/doi/10.1085/jgp.200810079

Supplemental Material can be found at:
http://jgp.rupress.org/content/suppl/2009/02/22/jgp.200810079.DC1.html

Published February 23, 2009

this 12-residue length also corresponds to the minimal linker length between the β2 subunit transmembrane segment 1 (TM1) and the FIW epitope that is required for an N terminus to be inactivation competent (Xia et al., 2003). Together, these results suggest that, over the length spanned by the 12-residue segment between TM1 and the binding site of the FIW motif within the central cavity, basic residues are protected from digestion by trypsin. However, for digestion of N termini when channels are closed, the time course of trypsin-mediated digestion of β2 N termini was described by a power term, *n*, of ∼2.0–2.5 (see Eq. 1 in Materials and methods). For the simple case in which all N termini are equally digestible by trypsin, the digestion process should exhibit a power term of 4. To explain a power term of $n = 2.0–2.5$, it was therefore proposed that, with channels mainly closed, not all N termini are equally accessible to digestion by trypsin, perhaps because some N termini are transiently protected from digestion by occupancy of an antechamber. To account for the observations a model was proposed (Fig. 2 A, Scheme 1) in which, even for closed channels, only one of the four N termini can occupy the protected volume at a time.

Although the antechamber occupancy model accounts well for the key features of the earlier data, the idea that some N termini can be protected from digestion in closed channels depends largely on the observation of a power term <4. An untested prediction of the model is that, if the occupancy time in the antechamber could be reduced, the overall digestion time course should be two- to fivefold faster with an associated increase in the value of *n* (Zhang et al., 2006). Here, we provide additional support for this idea through three approaches. First, to assess whether specific determinants of the β2 N terminus are responsible for protection when channels are closed, we examined mutated β subunit N termini. Second, to assess whether pore occupancy and antechamber occupancy involve distinct binding events, we examined the ability of cytosolic quaternary blockers to speed up the digestion time course. Third, to assess whether there

TABLE I

Sequences of the Human β2 N Terminus and Mouse Wild-type and Mutated β3 N Termini

	1	11	21	31	41
hβ2	MFIWTSGRTS	SSYRHDEKRN	IYQKIRDHDL	LDKRKTVTAL	– – –KAGEDRAILL
mβ3a	MQPFSIPVQI	TLQGGRRRQG	RTALPASGKI	NGDPLKVHPK	LPSSAGEDRAMLL
mβ3b	M – – – – – – –	– – – – – TALPA	SGK – – – – – I	NGDPLKVHPK	LPSSAGEDRAMLL
hβ3b	M – – – – – – –	– – – – –TAFPA	SGKKRETDYS	DGDPLDVHKR	LPSSTGEDRAVML
mβ3a	MQPFSIPVQI	TLQGGRRRQG	RTALPASGKI	NGDPLKVHPK	LPSSAGEDRAMLL
mβ3aR16Q	MQPFSIPVQI	TLQGGQRRQG	RTALPASGKI	NGDPLKVHPK	LPSSAGEDRAMLL
mβ3aR17Q	MQPFSIPVQI	TLQGGRQRQG	RTALPASGKI	NGDPLKVHPK	LPSSAGEDRAMLL
mβ3aR18Q	MQPFSIPVQI	TLQGGRRQQG	RTALPASGKI	NGDPLKVHPK	LPSSAGEDRAMLL
mβ3aR16-18Q	MQPFSIPVQI	TLQGGQQQQG	RTALPASGKI	NGDPLKVHPK	LPSSAGEDRAMLL
mβ3aR16-18Q,R21Q	MQPFSIPVQI	TLQGGQQQQG	QTALPASGKI	NGDPLKVHPK	LPSSAGEDRAMLL
mβ3aR16-18Q,R21Q,K29Q	MQPFSIPVQI	TLQGGQQQQG	QTALPASGQI	NGDPLKVHPK	LPSSAGEDRAMLL
mβ3aK36Q,K40Q	MQPFSIPVQI	TLQGGRRRQG	RTALPASGQI	NGDPLQVHPQ	LPSSAGEDRAMLL
mβ3aK29Q,K36Q,K40Q	MQPFSIPVQI	TLQGGRRRQG	RTALPASGKI	NGDPLQVHPQ	LPSSAGEDRAMLL
mβ3aR16	MQPFSIPVQI	TLQGGRQQQG	QTALPASGQI	NGDPLQVHPQ	LPSSAGEDRAMLL
mβ3aR17	MQPFSIPVQI	TLQGGQRQQG	QTALPASGQI	NGDPLQVHPQ	LPSSAGEDRAMLL
mβ3aR18	MQPFSIPVQI	TLQGGQQRQG	QTALPASGQI	NGDPLQVHPQ	LPSSAGEDRAMLL
mβ3aR21	MQPFSIPVQI	TLQGGQQQQG	RTALPASGQI	NGDPLQVHPQ	LPSSAGEDRAMLL
mβ3aR18,R21	MQPFSIPVQI	TLQGGQQRQG	RTALPASGQI	NGDPLQVHPQ	LPSSAGEDRAMLL
mβ3aR16-18Q	MQPFSIPVQI	TLQGGQQQQG	RTALPASGKI	NGDPLKVHPK	LPSSAGEDRAMLL
mβ3aR16-18Q,R21Q	MQPFSIPVQI	TLQGGQQQQG	QTALPASGKI	NGDPLKVHPK	LPSSAGEDRAMLL
mβ3aR16-18Q,R21Q,K29Q	MQPFSIPVQI	TLQGGQQQQG	QTALPASGQI	NGDPLKVHPK	LPSSAGEDRAMLL
FIW-20Q-2K-8Q-β2		MFIWQQQQQQ	QQQQQQQQQQ	QQQQ–KKQQQ	QQQQQRAILL
FIW-20Q-3K-8Q-β2		MFIWQQQQQQ	QQQQQQQQQQ	QQQQ-KKKQQQ	QQQQQRAILL
FIW-20Q-4K-8Q-β2		MFIWQQQQQQ	QQQQQQQQQQ	QQQQKKKKQQQ	QQQQQRAILL
FIW-8Q-2K-20Q-β2		MFIWQQQQQQ	QQ–KKQQQQ	QQQQQQQQQQQ	QQQQQRAILL
FIW-8Q-3K-20Q-β2		MFIWQQQQQQ	QQ-KKKQQQQ	QQQQQQQQQQQ	QQQQQRAILL
FIW-8Q-4K-20Q-β2		MFIWQQQQQQ	QQKKKKQQQQ	QQQQQQQQQQQ	QQQQQRAILL

The beginning of the first transmembrane segment is underlined. The bottom three are examples of artificial N termini.

Published February 23, 2009

are β subunit–specific determinants of fractional occupancy within the antechamber, we examined the trypsin sensitivity of other β subunit N termini. Overall, the results provide additional validation for the idea that binding of an N terminus within a protected antechamber provides protection against digestion by trypsin. We also address the issue of whether such protection arises because basic residues are physically hidden from attack by trypsin within the antechamber or whether binding of the N terminus places structural constraints on the basic residues, thereby reducing attack by trypsin.

MATERIALS AND METHODS

Oocyte Removal and Culture

Stage IV *Xenopus laevis* oocytes were injected with cRNA as described previously (Xia et al., 1999, 2002). mSlo1 α and β subunit cRNA were prepared at ~1 μg/μl. Typically, the α cRNA was initially diluted to 1:20 by volume, and then the injection solution was prepared at cRNA ratios of 1:2 (α/β). For some constructs, the relative amount of β subunit cRNA was increased to ensure full stoichiometric assembly of α and β subunits. Currents were typically recorded within 3–5 d after cRNA injection.

Constructs and Mutations

The mSlo1 construct (GenBank accession no. NP_034740) was originally obtained from L. Salkoff (Washington University School of Medicine, St. Louis, MO) and is identical to that in earlier work (Xia et al., 1999, 2002). The wild-type human β2 subunit (GenBank accession no. NP_852006) was as described previously (Xia et al., 1999). Preparation of new hβ2 N-terminal mutations followed previously published procedures (Xia et al., 2003). The mouse β3a subunit was assembled from expressed sequence tags based on exons defined in the mouse genome (Zeng et al., 2008). Table I lists N-terminal sequences for many constructs generated for this project along with the wild-type human β2, mouse β3a, and mouse and human β3b N termini.

Electrophysiology

Currents were recorded from inside-out patches (Hamill et al., 1981) using an Axopatch 200 amplifier (MDS Analytical Technologies) with stimulation protocols and data acquisition under control of the Clampex program (MDS Analytical Technologies). Recording pipettes used borosilicate capillary tubes, had resistances of 1–3 MΩ's after fire polishing, and were coated with Sylgard 184 (Dow Corning). During seal formation, oocytes were maintained in frog ringer (in mM: 115 NaCl, 2.5 KCl, 1.8 $CaCl_2$, and 10 HEPES, pH 7.4). The pipette/extracellular solution was as follows (in mM): 140 K-methanesulfonate, 20 KOH, 10 HEPES, and 2 $MgCl_2$, pH 7.0. The solution used for bathing the cytosolic membrane contained 140 mM potassium methanesulfonate, 20 mM KOH, 10 mM HEPES(H^+), and one of the following: 5 mM EGTA (for nominally 0 Ca^{2+}) or 5 mM HEDTA (with Ca^{2+} added to make 10 μM free Ca^{2+}). A Ca^{2+}-sensitive electrode was used to calibrate the 10 μM solution by comparing it to commercial Ca^{2+} solutions (World Precision Instruments). Solutions were applied to patches through a continuously flowing stream with a multibarrel local application system. The experimental temperature was ~22–25°C. *N*-(4-[benzoyl]benzyl)-*N,N,N*-tributylammonium bromide (bbTBA) was obtained from Spectra Group Limited. Other chemicals were from Sigma-Aldrich.

Trypsin Application Methods

Trypsin was from porcine pancreas (chymotrypsin, <1 unit/mg protein; type IX-S; Sigma-Aldrich). Previous work established that digestion of β2 N termini by trypsin reflects an action at basic residues, indicative that contamination by other enzymes is minimal (Zhang et al., 2006). A β2 N terminus in which all basic residues were neutralized to Q (β2-10Q) exhibits no digestion by trypsin over the time course of these experiments (Zhang et al., 2006).

The trypsin application procedures are as described previously (Zhang et al., 2006). In brief, peak and steady-state BK current activated by 10 μM Ca^{2+} was monitored by 200-ms test steps to +140 mV after a 30–50-ms preconditioning step to −140 mV. Between test steps, trypsin was applied for timed intervals while the patch was maintained in conditions that bias the channel-gating equilibrium. The three test conditions used were: (1) 0 Ca^{2+}, 0 mV (channels are closed); (2) 0 Ca^{2+}, −80 mV (channels are closed; the more negative holding potential was necessary for some mutated constructs); and (3) 10 μM Ca^{2+}, 0 mV (channels are mostly inactivated). Although trypsin was applied for precisely timed intervals, the exact time course of wash-in and washout of trypsin from the patch is unknown. Care was taken to ensure that each patch was maintained in the particular test condition (voltage and Ca^{2+}) for at least 15 s before and after trypsin application, before test steps to monitor BK status were initiated. When effects of quaternary ammonium blockers on digestion time course were evaluated, blockers were applied at the beginning and end of a particular test condition for a period that preceded the onset of trypsin application and persisted after washout of trypsin. This ensured that blocker occupancy was at steady state both before and after trypsin application.

Data Analysis

Current waveforms were analyzed either with Clampfit (MDS Analytical Technologies) or with programs written in this laboratory. The time course of removal of inactivation was fit with the following function (Zhang et al., 2006):

$$I(t) / I_{max} = (1 - \exp(-t / \tau_d))^n, \quad (1)$$

where I_{max} is the maximal peak outward current observed after removal of inactivation, τ_d is the time constant of the process, and n is a power factor. This function postulates that inactivation arises from the binding of a single inactivation domain, but that n domains must be cleaved by trypsin to remove inactivation (Ding et al., 1998; Wang et al., 2002; Zhang et al., 2006). The application of this equation has been considered in more detail previously (Zhang et al., 2006). In some constructs, studied under inactivating conditions, inactivation was incompletely removed even at the end of ~15 cumulative minutes of trypsin digestion. In such cases, the peak current measured during test steps was not a good measure of I_{max} and, thus, the empirically observed I_{max} in an individual experiment would result in an inappropriately rapid digestion time course. In such cases, the true I_{max} was therefore estimated by the fold increase in peak current defined for a set of patches from a given construct studied when channels are largely closed.

Modeling of Trypsin-mediated Removal of Inactivation

As before (Zhang et al., 2006), the trypsin-mediated removal of inactivation was modeled with the macroscopic simulation capabilities of the QUB software suite (http://www.qub.buffalo.edu/wiki/index.php/Main_Page). Gating parameters used here were as described (Zhang et al., 2006) and are based on previous studies of BK activation and inactivation. Here, we extend the simulations to examine the consequences of changes in the affinity of binding within the antechamber and binding within the central cavity. Furthermore, we consider a two-site protection model.

In earlier work, we determined predicted digestion time constants, τ_d, and power terms, n, for a one-site protection model as a function of fractional occupancy of that site (Fig. 6 E from

Published February 23, 2009

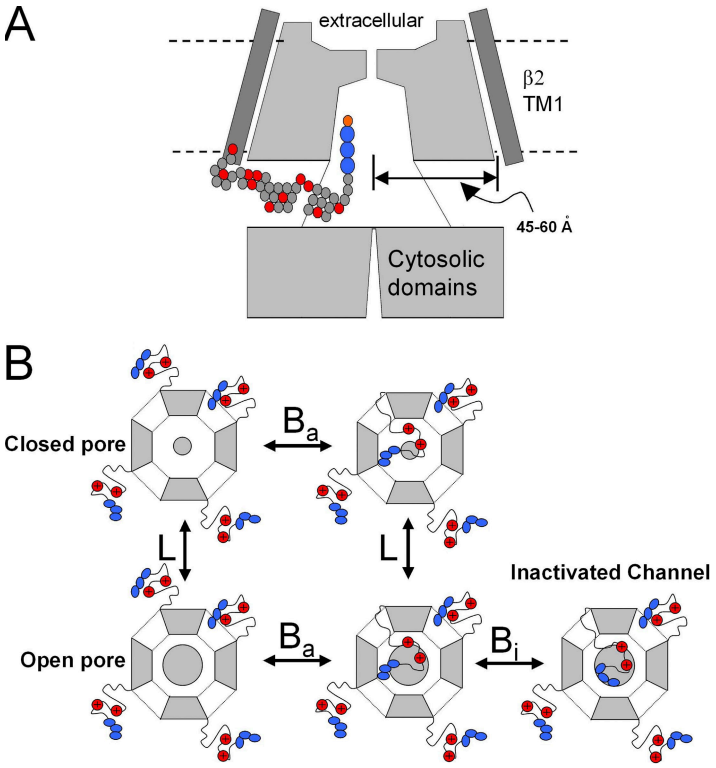

Figure 1. Cartoons summarizing the idea of antechamber occupancy and lateral access of β2 N termini to the BK channel pore. (A) The pathway for access of the β2 N-terminal inactivation domain to the BK channel central cavity is schematized. N termini must enter the central cavity by passing through the side portals separating the BK channel pore domain from the cytosolic domains involved in Ca^{2+} binding. The lateral distance from the center of the pore to the position where the N terminal attaches to the β2 subunit TM1 domain is estimated to be ∼45–60 Å (Zhang et al., 2006). Each ball in the schematized N terminus represents an amino acid, with red indicating basic residues and blue indicating the FIW hydrophobic triplet essential for inactivation. (B) Cartoons schematically summarize proposed configurations of β2 N termini during gating and inactivation. Each channel contains four β2 subunits (containing a triplet of hydrophobic residues [blue] at the N terminus and two digestible basic residues, R8 and R19 [red]), each of which can potentially enter the channel antechamber (equilibrium, B_a) through side portals. The central pore is indicated by the shaded, inner circle (smaller, closed channel; larger, open channel). In this scheme, only one N terminus can occupy the antechamber at a time. Channels open in accordance with equilibrium constant L. Open channels with a β2 N terminus in the antechamber may also inactivate (equilibrium constant, B_i).

Zhang et al., 2006). We have now determined that the calculation of fractional occupancies in the earlier plot contained an error. However, the relationship between fractional prolongation of τ_d and n at different occupancies was correct and is identical to that reported here (Fig. 12, B and C). This error does not alter the conclusion that increases in fractional occupancy at the site of protection slow τ_d and reduce n.

Online Supplemental Material

This manuscript contains additional material that provides further examples of the factors that contribute to accessibility of N-terminal domains to digestion by trypsin. In Fig. S1, the ability of a Kvβ2 N terminus to influence digestion by trypsin is illustrated. In Fig. S2, the trypsin digestibility of hβ3a and hβ3b are compared. In Figs. S3 and S4, the basic residues that are attacked by trypsin in the mβ3a N terminus are defined. In Fig. S5, the failure of the β2 FIW motif to slow digestion of the β3a N terminus is examined. The online supplemental material is available at http://www.jgp.org/cgi/content/full/jgp.200810079/DC1.

RESULTS

Scheme 1 (Fig. 2 A) encapsulates the proposal that a single β subunit N terminus can transiently occupy a position protected from digestion by trypsin before moving to a position of inactivation. This model ignores the cases in which inactivation may occur directly without transient binding in the antechamber. The consequences of that omission are considered below. Fig. 2 (B–G) displays several predictions of this model based on parameters given in Table II. In Fig. 2 B, the basic expectations for Scheme 1 are shown both for closed-channel conditions and inactivating conditions. These predictions mirror previous experimental results and analysis (Zhang et al., 2006). For closed-channel conditions, we mean those conditions of Ca^{2+} and voltage under which channels are predominantly in closed states alone, whereas by inactivating conditions we mean those conditions of voltage and Ca^{2+} where channels are almost exclusively in inactivated states. For inactivating conditions, the model predicts that the trypsin-mediated removal of inactivation is markedly slowed with the resulting power term, n, approaching 1.0, consistent with the idea that a single N terminus is protected during inactivation. We presume that protection during inactivation represents binding of a single N terminus to a position within the BK central cavity. If the affinity for binding within the antechamber is reduced (Fig. 2 C), both the digestion time course under closed-channel conditions is faster and the steepness of the digestion time course, n, is increased. This increase in n depends solely on the affinity of an N terminus for antechamber site and not on the overall rate of the digestion process (Fig. 2 D); when the effective rate is varied by changing the relative trypsin concentration, n is unaffected and the measured apparent rate of digestion varies linearly with trypsin concentration (Fig. 2 E). When binding in the central cavity is altered (Fig. 2 F), closed-channel protection is unaffected, but the protection conferred by inactivation is markedly reduced. In the illustrated example, protection produced by inactivation is almost abolished, even when current inactivates to a level that is <20% of the peak current. Finally, when the affinities for both the central cavity site and the antechamber site are reduced (Fig. 2 G), shifts in both closed-channel

Published February 23, 2009

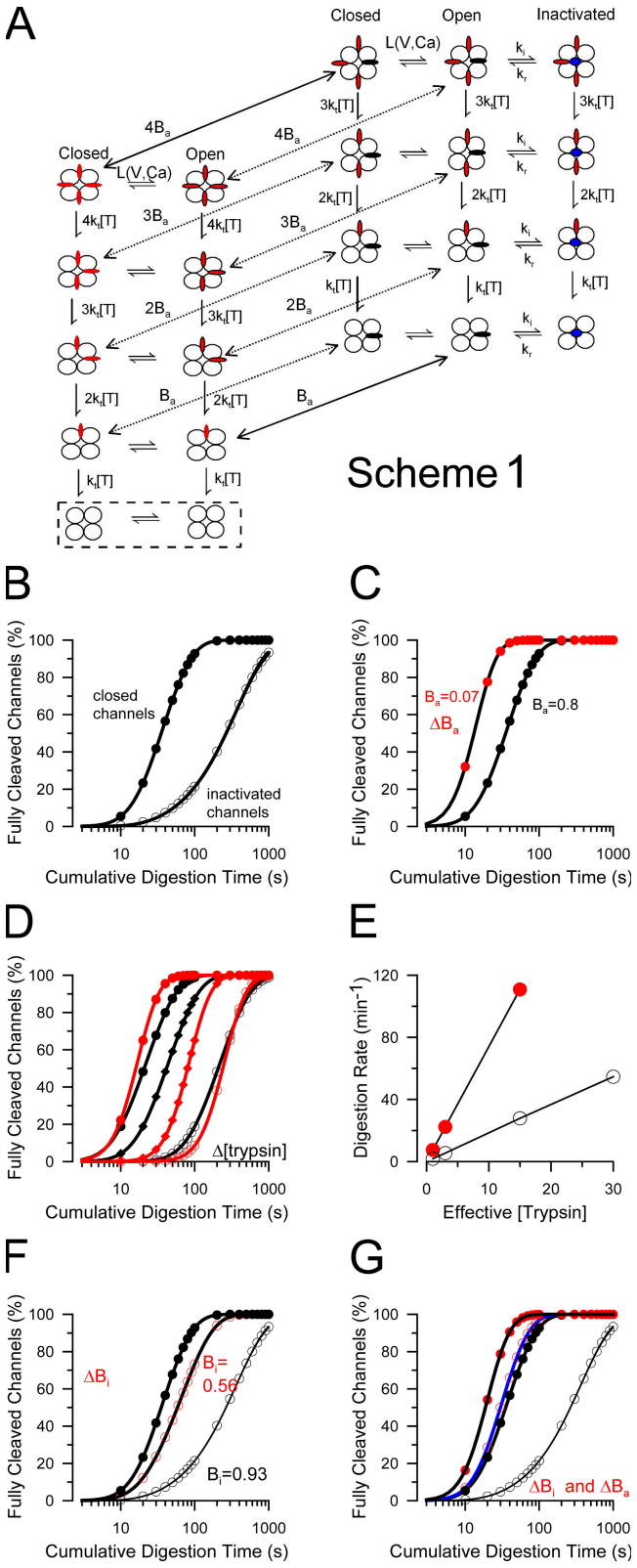

Figure 2. Stochastic model for protection of β2 N termini from digestion by trypsin. (A) A kinetic scheme describing the proposed digestion of β2 N termini by trypsin is shown, including channel gating (L(V, Ca)), protection of N termini within the antechamber (P), and inactivation. States highlighted in the box are those in which inactivation has been completely removed by trypsin. Flattened red ovoids correspond to N termini in positions outside the antechamber, while, when black, are within the antechamber. Blue circles on the axes of the pore correspond to an N terminus in an inactivation position. (B–G) Simulated digestion time courses based on this scheme. (B) The simulated digestion time courses are shown for parameters given in Table II for closed-channel conditions (Po = 0.01) or inactivating conditions (Po = 0.99; B_i = 0.93). The fit of Eq. 1 to the time course under closed-channel conditions yielded τ_d = 28.5 s (n = 2.09). Under inactivating conditions, τ_d = 327.3 s (n = 1.17). (C) The affinity of the N terminus for the site involved in closed-channel protection (affinity for antechamber, B_a) was reduced by increasing the dissociation rate from the site 50-fold. Under these conditions (red circles), τ_d = 7.2 s (n = 3.98). (D) The effective digestion rate was varied (approximating changes in [trypsin] [black symbols]) for closed-channel conditions as defined in A and for the case that antechamber binding affinity is reduced (red symbols). With reduced antechamber binding affinity, the slope of the digestion time course is steeper, but the slope is unaffected by the effective rate of the digestion process. (E) The effective digestion rates are plotted as a function of effective trypsin concentration for the cases of modest closed-channel protection (open circles) or without such closed-channel protection (red circles). The slope of the lines shows the approximately fourfold difference in effective digestion rate that arises because of the difference of occupancy in the antechamber, despite the fact that the same underlying molecular rate for the cleavage step was used in the two cases. (F) The effect of weakening the affinity of the inactivation domain for the channel pore (ΔB_i) is illustrated. The rate of dissociation of the inactivation domain from its blocking position was increased 10-fold, changing steady-state inactivation from 0.93 to 0.56. In this case, under inactivating conditions, the digestion time course (red circles) approaches that observed for closed-channel conditions (solid black circles) with τ_d = 55.8 s (n = 1.63), whereas under there is no difference between the two cases for closed-channel conditions (not depicted). (G) The effect of a fivefold weakening of both binding in the antechamber (B_a) and at the inactivation site (B_i) is shown. This alters digestion both under closed-channel conditions (solid symbols; τ_d = 11.1 s; n = 3.43) and under inactivated conditions (open symbols; τ_d = 21.7 s; n = 2.45). Values for simulations and resulting measurements of τ_d and n are given in Table II.

protection and inactivated-mediated protection are predicted. These examples illustrate the varieties of behaviors in the digestion time course that might be expected as mutations of β2 N termini are examined. It should be noted that many of these predictions are not unique to a one-site protection model but are qualitatively characteristic of any model in which there is protection involving less than the full set of four N-terminal domains. Inclusion in Scheme 1 of a direct transition from open to inactivated states, thereby bypassing the antechamber binding site, has no impact on the predicted digestion behavior under closed-channel conditions, but will impact on the predicted digestion time course under inactivating conditions, dependent on various equilibrium constants. However, the basic idea that binding in the central cavity will slow digestion will apply regardless of the details of the relationship between central cavity and antechamber binding.

Published February 23, 2009

TABLE II

Simulations of Effect of Antechamber Binding and Inactivation on the Time Course of Trypsin-mediated Removal of Inactivation in Accordance with Scheme 1

Condition	Po	k_i	k_r	B_i	p_f	p_r	B_a	k_t	τ_d (s)	*n*
		s^{-1}	s^{-1}	$\frac{k_i}{k_i + k_r}$	s^{-1}	s^{-1}	$\frac{p_f}{p_f + p_r}$	s^{-1}		
Fig. 2 B										
Closed channels	0.01	12.5	50	0.2	8,000	2,000	0.8	0.15	28.5	2.09
Inactivated	0.99	12.5	1	0.93	8,000	2,000	0.8	0.15	327.3	1.17
Fig. 2 C ΔPa										
Closed channels	0.01	12.5	50	0.02	8,000	100,000	0.07	0.15	7.2	3.98
Fig. 2 (D and E) Vary k_t										
Pa = 0.286	0.01	0.125	50	0.0025	8,000	20,000	0.286	0.15	9.0	3.74
	0.01	0.125	50	0.0025	8,000	20,000	0.286	0.03	44.8	3.78
	0.01	0.125	50	0.0025	8,000	20,000	0.286	0.01	133.3	3.82
Pa = 0.842	0.01	0.125	50	0.0025	8,000	1,500	0.842	0.3	18.3	1.85
	0.01	0.125	50	0.0025	8,000	1,500	0.842	0.15	35.9	1.89
	0.01	0.125	50	0.0025	8,000	1,500	0.842	0.03	183.8	1.84
	0.01	0.125	50	0.0025	8,000	1,500	0.842	0.01	540.2	1.88
Fig. 2 F ΔPi										
Inactivated	0.99	12.5	10	0.56	8,000	2,000	0.8	0.15	55.8	1.63
Fig. 2 G ΔPi && ΔPa										
Closed channels	0.01	12.5	50	0.2	8,000	10,000	0.44	0.15	11.1	3.43
Inactivated	0.99	12.5	5	0.71	8,000	10,000	0.44	0.15	21.7	2.45

Po is the open probability defined by the closed-open equilibrium constant, L. k_i is the forward rate of block by a single inactivation domain, with k_r, the unblocking rate. B_i reflects the fractional occupancy of the inactivation binding site conditions of high Po and saturation of the antechamber site. p_f and p_r are rates of binding and unbinding of an N terminal to the proposed antechamber site, with B_a reflecting the fractional occupancy of the antechamber. k_t is the rate of digestion of a single N terminus. τ_d and *n* are the digestion time constant and power terms from fits of Eq. 1 to the digestion time course simulated with the given parameters. Because Eq. 1 is not an explicit derivation of the model used for simulation, τ_d and *n* are not exact values, but the confidence limits on the fitted values were typically <1–4%.

It should also be kept in mind that protection of basic residues that occurs because of binding of N termini within the antechamber might arise from distinct mechanistic reasons. On one hand, binding in the antechamber of a portion of the N terminus may simply place basic residues within the antechamber making them inaccessible to digestion. Alternatively, binding of part of the N terminus in the antechamber may leave basic residues outside the boundaries of the antechamber, but the ability of trypsin to digest a freely mobile N terminus or a tethered N terminus may differ. In both cases, binding of a portion of the N terminus within the antechamber is required to achieve values of $n << 4$. However, whether closed-channel protection involves binding in the antechamber remains a hypothesis that the present results are designed to test.

A Mutation in the FIW Motif Speeds up Digestion under Closed-Channel Conditions and Increases the Power Term

Here, we test the idea that under closed-channel conditions a β2 N terminus can transiently occupy a position that protects it from digestion by trypsin. First, the model predicts that if the fractional time that a β2 N terminus spends within the antechamber is decreased, the digestion time course should become faster. Second, if protection when channels are closed is sufficiently reduced, then *n*, the power term of the digestion time course, should approach 4. The initial hydrophobic sequence (MFIW) of the β2 N terminus, which is critical for inactivation (Xia et al., 2003), might influence residency time within an antechamber by interacting with other hydrophobic residues. We therefore examined β2 mutations either within or near the hydrophobic FIW triplet to determine whether any such manipulations might alter the time course of digestion by trypsin.

We first examined a construct in which tryptophan in position 4 was mutated to glycine (W4G). Inactivation is maintained in this construct, although with less steady-state block and more rapid unblock (Xia et al., 2003). The ability of trypsin to remove inactivation was examined by measuring BK currents before and after brief trypsin applications, as described previously (Zhang et al., 2006). Inactivation of α+β2(W4G) was so rapidly removed by 0.1 mg/ml trypsin that a time course could not be quantitatively defined. Reducing the trypsin

Published February 23, 2009

concentration to 0.01 mg/ml resulted in a removal of inactivation that could be compared with digestion of the wild-type β2 N terminus (Fig. 3, A and B). An effective rate of digestion was calculated based on the trypsin concentration and the measured digestion time constant. For wild-type β2, the effective rate was 0.7 (±0.05) × 10^4 M^{-1} s^{-1}, whereas for W4G the rate was 5.4 (±0.2) × 10^4 M^{-1} s^{-1}, for an overall seven- to eightfold faster digestion of W4G (also see Fig. 11). Thus, although both wild-type β2 and W4G contain the same trypsin-digestible basic residues (R8 and R19), under closed-channel conditions the W4G construct is much more readily digested by trypsin. This unambiguously indicates that the tryptophan in position 4 stabilizes some conformation or position of the β2 N terminus that protects basic residues from attack by trypsin.

Another important aspect of the W4G digestion time course was that the fit to the digestion time course required a power term, *n*, that was clearly steeper than that for digestion of β2 currents (Fig. 3 E). For W4G, $n = 3.45 \pm 0.13$, whereas, for β2, $n = 2.23 \pm 0.39$. Plotting the digestion time course on a log-log scale illustrates clearly the steeper digestion time course for the W4G construct. This result supports the model of Fig. 2 A because *n* approaching 4 can only be obtained in cases when all N termini can be similarly attacked by trypsin (Zhang et al., 2006). The change in the power term indicates that the difference in digestion between wild-type β2 and W4G arises not because of a change in conformation that occurs in all N termini, but rather from disruption of occupancy of site(s) of protection possibly within the antechamber.

We also examined digestion of W4G under conditions in which channels are largely inactivated (10 μM Ca^{2+}, +80 mV; Fig. 3, C and D). For the W4G construct, conditions that promote inactivation failed to protect against digestion by trypsin. We attribute this largely to the fact that, in contrast to wild-type β2, the level of steady-state current for W4G at 10 μM Ca^{2+} and +80 mV is substantial (I_{ss} at +80 mV is ~10–25% of the maximal conductance at +80 mV), such that the residency time of any N terminus within its inactivating position is brief. This is consistent with the predicted absence of inactivation-associated protection when the inactivation affinity is reduced (Fig. 2 F).

Collectively, the faster digestion τ_d and the steeper power term are consistent with the idea that W4G N termini only transiently bind within the antechamber, such that all N termini can be readily digested. The fold increase in τ_d observed between wild-type β2 and W4G

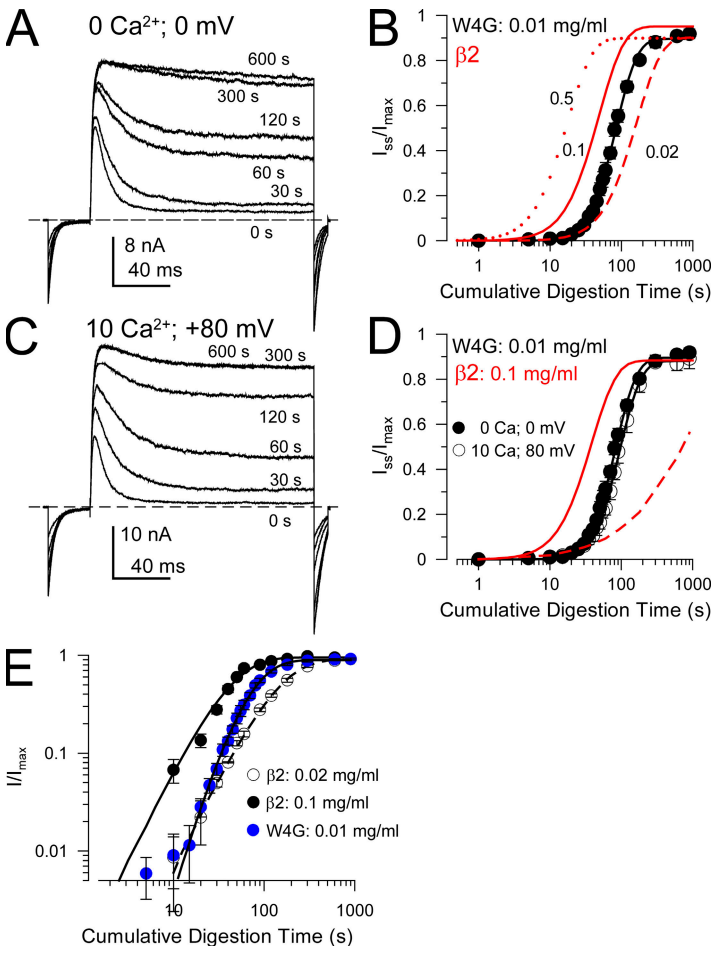

Figure 3. The W4G mutation in the β2 FIW motif speeds up trypsin-mediated removal of inactivation under closed-channel conditions. (A) Currents resulting from α + β2(W4G) channels were activated by depolarizing steps to +80 mV with 10 μM Ca^{2+}. Between voltage steps, the patch was held at 0 mV with 0 Ca^{2+} and 0.01 mg/ml trypsin was applied for defined periods of time. Times given on the panel are the cumulative time of trypsin application. (B) The time course of digestion of β2-W4G under closed-channel conditions with 0.01 mg/ml trypsin (black circles and line) is compared with the digestion of β2 wild type with 0.02, 0.1, and 0.5 mg/ml trypsin (red lines). (C) Similar test traces are shown for a patch in which trypsin was applied in the presence of 10 μM Ca^{2+} at +80 mV, a condition in which β2-(W4G) channels are >95% inactivated. (D) The time course of removal of inactivation is plotted for sets of patches for the conditions shown in A and C. For comparison, the solid red line and dotted red line correspond, respectively, to the digestion of wild-type β2 N termini under closed-channel conditions (0 μM Ca^{2+}; 0 mV) with 0.1 mg/ml trypsin and under inactivating conditions (10 μM Ca^{2+}; 0 mV) with 0.1 mg/ml trypsin. (E) The time course of digestion of β2 and β2-W4G N termini is plotted on a log-log scale to compare the slope of the digestion process. For these fits, the power term for β2 digestion was 2.23 ± 0.39, and for β2-W4G it was 3.45 ± 0.13.

Published February 23, 2009

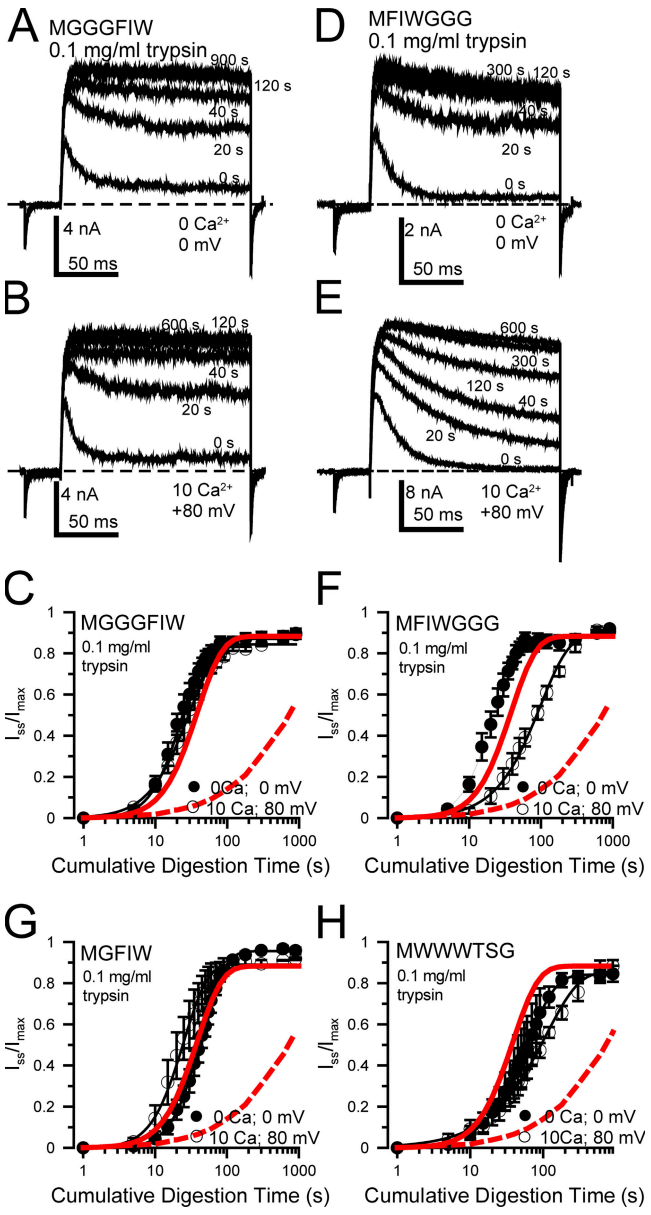

Figure 4. Some manipulations of the β2 N terminus can alter inactivation-dependent protection against digestion, with minimal effects on rates of digestion during closed-channel conditions. (A) Traces show digestion at different times by 0.1 mg/ml trypsin applied in the presence of 0 Ca^{2+} at 0 mV (closed-channel conditions) for the MGGGFIW construct. Displayed currents were obtained between trypsin applications with 10 μM Ca^{2+} as in Fig. 3. (B) Traces are shown for the MGGGFIW construct during digestion by 0.1 mg/ml trypsin in 10 μM Ca^{2+} at +80 mV (inactivated conditions). For this construct, at +80 mV, the steady-state non-inactivating current is ∼30–40% of the maximal current. (C) The digestion time courses for MGGGFIW are plotted for the two conditions (black symbols, closed channel; open symbols, inactivated), along with the fitted results for the wild-type β2 subunit (dashed red line, inactivated conditions [10 μM Ca^{2+}; 0 mV]; red line, closed-channel conditions [0 Ca^{2+}; 0 mV]). (D and E) Traces are shown for the MFIWGGG construct for digestion by 0.1 mg/ml trypsin either at 0 Ca^{2+}, 0 mV (D) or at 10 μM Ca^{2+}, +80 mV (E). For MFIWGGG, the steady-state non-inactivating current at +80 mV is ∼5% of the maximal current. (F) Digestion time courses are plotted for the MFIWGGG construct along with the time course for β2. (G and H) Digestion time courses are plotted for MGFIW (G) and MWWWTSG (H), both under closed-channel and inactivating conditions.

(seven- to eightfold) is somewhat greater than predicted by Scheme 1 (two- to fivefold) in which only a single N terminus can occupy the protected site at a time (Zhang et al., 2006). Given that the power term for W4G was 3.4, some protection against digestion may still persist under closed-channel conditions for this construct. This indicates that an N terminus with no closed-channel–associated protection would be digested even more rapidly.

Mutations Near the FIW Motif Disrupt Inactivation-associated Protection against Trypsin Digestion, but Have Little Effect on Digestion under Closed-Channel Conditions

We next examined several constructs in which the hydrophobic motif (FIW) or the hydrophobicity was maintained (WWW) while other alterations near this motif were made (Fig. 4). Constructs MGGGFIW (Fig. 4, A–C), MFIWGGG (Fig. 4, D–F), MGFIW (Fig. 4 G), and MWWWTSG (Fig. 4 H) all exhibited control digestion time courses with 0.1 mg/ml trypsin that were generally similar to that of wild-type β2, even though each construct differed substantially in the extent of steady-state inactivation observed at +80 mV and 10 μM Ca^{2+}. Thus, these changes in the β2 N terminus altered the apparent binding affinity of the inactivation domain for the central cavity binding site, but did not alter the time course of digestion by trypsin under closed-channel–associated conditions.

For MGGGFIW, there was little difference in the digestion time course either under closed-channel or inactivating conditions. This may arise because, at +80 mV, the steady-state current with 10 μM Ca^{2+} is ∼40% of the peak current (estimated from Xia et al., 2003), such that the duration of the inactivated state at +80 mV may be insufficient to produce protection. In contrast, MFIWGGG, for which the steady-state current at +80 mV with 10 μM Ca^{2+} is ∼5% of the peak current (Xia et al., 2003), does exhibit some inactivation-associated protection against digestion, although not as strong as for wild-type β2. Both MGFIW and MWWWTSG show only slight differences between digestion under closed-channel conditions and inactivating conditions, again perhaps reflecting the relative instability of the inactivated state. The time course of digestion for MWWWTSG is actually slower than for wild-type β2, with a shallower slope perhaps suggesting that the very hydrophobic WWW motif may enhance protection from digestion under closed-channel conditions. Overall, the extent to which inactivation-associated protection from digestion is reduced correlates with the amount of steady-state current relative to peak-inactivating current that is observed for a given construct at +80 mV and 10 μM Ca^{2+}.

Published February 23, 2009

Thus, in this case, channels may spend an appreciable fraction of time in open rather than inactivated states, such that protection from digestion is reduced.

These results indicate that the determinants that allow an N terminus to exhibit inactivation-associated protection can be dissociated from those that influence digestion under closed-channel conditions. This strongly supports the hypothesis that there are two distinct positions of binding of the N termini, one in a position associated with inactivation presumably in the central cavity and another possibly in the antechamber. The general behavior of these constructs can be rationalized within the context of Scheme 1 (Fig. 2 A), and the simulated behaviors (Fig. 2, B–G) accord with the basic idea that the affinities for the antechamber site and the inactivation site are independent.

Removal of residues FIW from the β2 N terminus results in a non-inactivating N terminus (Xia et al., 2003). Substitution of other inactivation-competent motifs might result in N termini that exhibited more rapid closed-channel digestion than wild-type β2 N termini. We created two constructs (Fig. S1A): one in which residues QVSIAR preceded the β2 FIW motif (KvβFIW), and a second one in which QVSIAR replaced the FIW motif (Kvβ2TSG). QVSIAS corresponds to the first six residues after the initiation of methionine of the Kvβ1.1 N terminus, an inactivation peptide of Kv1.2 (Zhou et al., 2001). Both constructs resulted in inactivation of BK channels with temporally distinct time courses (Fig. S1, B and D). For KvβFIW, the closed-channel digestion followed a time course virtually identical to wild-type β2 with 0.1 mg/ml trypsin (Fig. S1 C). This equivalence in digestion occurred despite the extra arginine residue that immediately preceded the FIW motif. In contrast, for the KvβTSG construct, the closed-channel digestion occurred with a rate similar to that of the β2-W4G construct (Fig. S1 E). We also made a similar construct in which residues QVSIAS replaced FIW motif to remove the extra positive charge. The digestion time course was somewhat slower than in the case of QVSIAR, but still severalfold faster than for the wild-type β2 N terminus (see summary in Fig. 11). These results again suggest that the FIW motif of β2 helps maintain protection against digestion under closed-channel conditions, perhaps by stabilizing occupancy within the antechamber. In addition, the KvβTSG construct exhibited a steeper digestion time course compared with β2 (n = 4.43 ± 0.39 vs. n = 2.23 ± 0.39; Fig. S1 E). This supports the idea that the digestion time course of the native β2 N termini under closed-channel conditions reflects the binding of N termini to some site of protection.

Quaternary Cytosolic Channel Blockers Do not Alter the Time Course of Removal of Inactivation by Trypsin under Closed-Channel Conditions

We hypothesized that cytosolic blockers of the BK central cavity might differentially affect the ability of trypsin to digest N termini under closed-channel conditions compared with those examined under conditions that favor inactivation. We first tested the ability of tetrabutylammonium (TBA), a BK channel pore blocker (Li and Aldrich, 2004), to alter rates of digestion of β2 N termini (Fig. 5). With 20 mM TBA, the trypsin digestion time course of β2 N termini was similar to that in the absence of TBA both for closed channels (0 Ca^{2+}, 0 mV) and for inactivated channels (10 μM Ca^{2+}, 0 mV; Fig. 5, A–C). The 0-voltage K_d for TBA block of BK channels has been estimated to be ∼0.5–1 mM (Li and Aldrich, 2004; Wilkens and Aldrich, 2006), with stronger block at more positive potentials ($z\delta$ = 0.21). Our experiments yield an estimate of the $K_d(0)$ for TBA block of ∼0.69 mM with $z\delta$ ∼0.12 (unpublished data). For a single-site blocking model, the fractional occupancy of the open channel at 0 mV is calculated to be ∼0.967 with 20 mM TBA and ∼0.986 for 50 mM TBA. It is therefore unlikely that the lack of effect of TBA reflects incomplete pore occupancy. This result is reminiscent of the inability of cytosolic channel blockers to compete with native BK β subunit N-terminal inactivation (Solaro et al., 1997; Xia et al., 1999; Lingle et al., 2001).

We next examined the ability of a bulky quaternary ammonium blocker, bbTBA, to influence β2 digestion by trypsin. bbTBA inhibits BK channels with a weakly voltage-dependent $K_d(0)$ of ∼5–10 μM with $z\delta$ of 0.15 (Wilkens and Aldrich, 2006), which is identical to our estimates of 5.0 μM and 0.11 (unpublished data). 1 mM bbTBA did not alter the trypsin-mediated removal of inactivation under closed-channel conditions but completely abolished the inactivation-associated protection against digestion (Fig. 5, D–F). Assuming single-site block of the open BK channel, the fractional occupancy by 1 mM bbTBA is calculated to be 0.995 at 0 mV.

We interpret these results as follows. It is known that the binding site for the rate-limiting step in inactivation mediated by the β2 N terminus is not inhibited by smaller quaternary ammonium blockers (Xia et al., 1999; Lingle et al., 2001). This presumably arises because of the two-step nature of the BK inactivation process in which the formation of a pre-inactivated open state precedes the transition to the inactivated state (Lingle et al., 2001; Benzinger et al., 2006). In this model ($C \rightleftharpoons O \rightleftharpoons O^* \rightleftharpoons I$), the transition to O* is the rate-limiting step in inactivation (Lingle et al., 2001). If small quaternary blockers bind equally well to both O and O*, they will have no impact on the apparent time course of the inactivation process. Thus, although TBA may occupy a pore-blocking position, it may not inhibit the ability of the N terminus to form the pre-inactivated open state. In contrast, bbTBA, by occupying a larger volume within the BK central cavity, apparently does impede the ability of β subunit N termini to reach a binding site. Finally, the inability of either TBA or bbTBA to substantially alter the rate of digestion by trypsin under closed-channel conditions supports

Published February 23, 2009

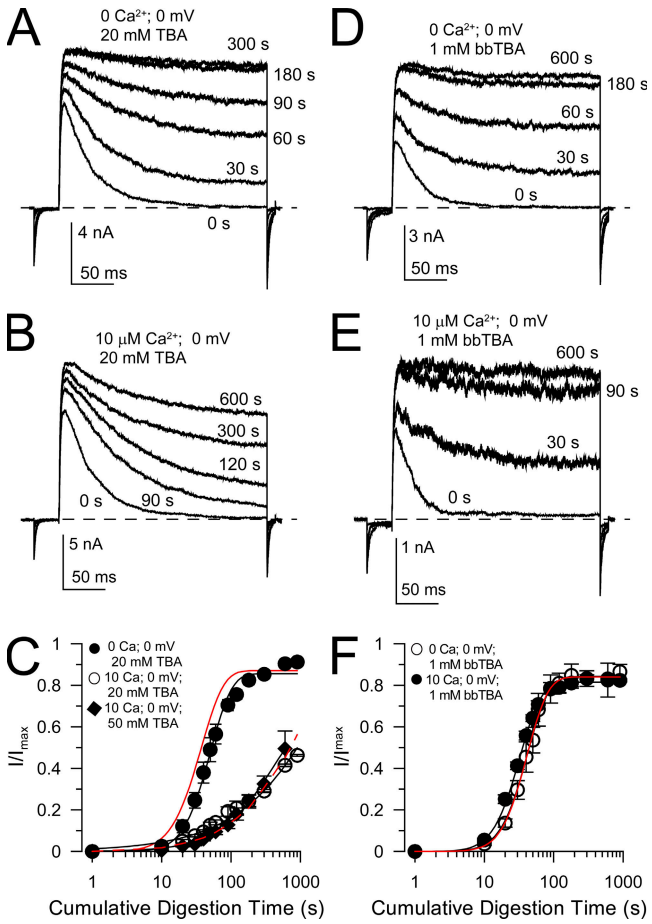

Figure 5. Inactivation-associated protection against digestion by trypsin is differentially sensitive to cytosolic channel blockers. (A) Traces show test sweeps at different time points during digestion of β2 by 0.1 mg/ml trypsin under conditions of low activation (0 Ca^{2+}; 0 mV) but in the presence of 20 mM TBA. (B) Traces show test sweeps during digestion of β2 by 0.1 mg/ml trypsin with 20 mM TBA under inactivating conditions (10 μM Ca^{2+}; 0 mV). (C) The time course of removal of inactivation is plotted for the indicated conditions. Neither 20 nor 50 mM TBA abolishes the inactivation-associated slowing of digestion. The red lines show the normal removal of inactivation of β2 subunits with 0.1 mg/ml trypsin in the absence of TBA for closed-channel (solid line) and inactivating (dotted line) conditions. (D) Traces show removal of β2-mediated inactivation by 0.1 mg/ml trypsin applied under closed-channel conditions, but with 1 mM bbTBA. (E) The digestion by 0.1 mg/ml trypsin occurred at 0 mV, 10 μM Ca^{2+}, with 1 mM bbTBA. (F) The time course of removal of β2-mediated inactivation is plotted for closed-channel and inactivating conditions, both with 1 mM bbTBA, showing the ability of bbTBA to prevent the inactivation-associated protection from digestion while not changing the digestion rate under closed-channel conditions.

the view that the site(s) of β2 interaction that is involved in defining closed-channel protection is distinct from any binding sites within the central cavity.

Trypsin Sensitivity of a Wild-type Mouse β3a Inactivation Domain greatly Exceeds that of the Wild-type Human β2 Inactivation Domain

N termini from different inactivating BK β subunits may differ in the rates of trypsin-mediated removal of inactivation based on differences in affinities for interaction within the antechamber. We therefore compared the trypsin sensitivity of inactivation mediated by the human β2 subunit (Fig. 6, A–C) with the mouse β3a subunit (Fig. 6, D–F). As with the β2-W4G construct, removal of inactivation mediated by β3a subunits with 0.1 mg/ml trypsin was so fast that a time course could not be readily defined. Reduction of the trypsin concentration to 0.01 mg/ml resulted in a removal of inactivation (Fig. 6, D–F) that followed a time course similar to digestion of the β2 N terminus by 0.1 mg/ml trypsin (Fig. 6, A–C). When trypsin was applied during inactivating conditions, the digestion of β3a N termini was slowed (Fig. 6 E), also similar to the behavior of β2 N termini (Fig. 6 B). In both cases, under inactivating conditions, the power term for the fit to the digestion time course approached one, consistent with the idea that the dissociation of a single N terminus becomes rate limiting for digestion by trypsin.

Time constants for digestion of mβ3a were determined at multiple trypsin concentrations (Fig. 7 A) and compared with previous estimates obtained for hβ2 (Zhang et al., 2006). For both subunits, the digestion rate was plotted as a function of [trypsin] (Fig. 7 B). For β3a, the digestion rate varied approximately linearly with [trypsin], with a slope of 9.97×10^4 M^{-1} s^{-1}. For β2 (Zhang et al., 2006), the limiting slope at low concentration was 6.82×10^3 M^{-1} s^{-1}, suggesting that there is a >10-fold difference between the digestion rates. Another important difference was that the power term in the fit to the removal of inactivation of mβ3a currents was clearly steeper than for β2 currents (Fig. 7 C), except with the highest tested trypsin concentration. As with β2, TBA and bbTBA had differential effects on inactivation-associated protection against β3a N-terminal digestion (Fig. 8). Whereas TBA was without effect on inactivation-associated protection (Fig. 8, A and B), bbTBA abolished the protection produced by inactivation (Fig. 8, C and D). No clear effects on closed-channel digestion were produced by either TBA or bbTBA.

We also examined the trypsin-mediated removal of inactivation of other N termini. The time course of removal of inactivation by 0.1 mg/ml trypsin for both hβ3a and hβ3b N termini is comparable to, but somewhat slower than, for digestion of hβ2 (Fig. S2).

Determinants of Digestion Rates of the β3a N Terminus

The faster digestion of the β3a N terminus with steeper digestion time course is consistent with the idea that, under closed-channel conditions, the β3a N terminus may have a reduced occupancy of the antechamber compared with the β2 N terminus. However, one might imagine other explanations. For example, the β3a N terminus may contain a greater number of accessible basic residues than the β2 N terminus.

Effects of mutations of basic residues in the β3a N terminus on the trypsin sensitivity were therefore examined (see Fig. 11 for summary and Table I for constructs).

Published February 23, 2009

The β3a N terminus contains four basic residues, R16–18 and R21 (Table I), arising from the β3a-specific N terminus, and then three other basic residues, K29, K36, and K40, shared in common with the β3b N terminus. We first examined constructs in which multiple basic residues were simultaneously neutralized. Mutation of K29Q, K36Q, and K40Q, or only K36Q and K40Q, resulted in constructs that were digested only slightly more slowly than wild-type β3a (Fig. S3 A). In contrast, mutation of R16–18Q and R21Q resulted in an inactivating construct that was hardly affected over 15 min of application of 0.1 mg/ml trypsin (Fig. S3 B). When only R16–R18 were neutralized to Q, digestion with 0.01 mg/ml trypsin persisted, although it was shifted (τ_d = 91.6 ± 9.6 s) several-fold relative to wild-type β3a (23.7 ± 1.4 s). Because K29, K36, and K40 contribute negligibly to digestion by trypsin, this suggests that residue R21 is at least one likely target of trypsin action.

We next examined constructs in which only a single basic residue was mutated or a single basic residue was

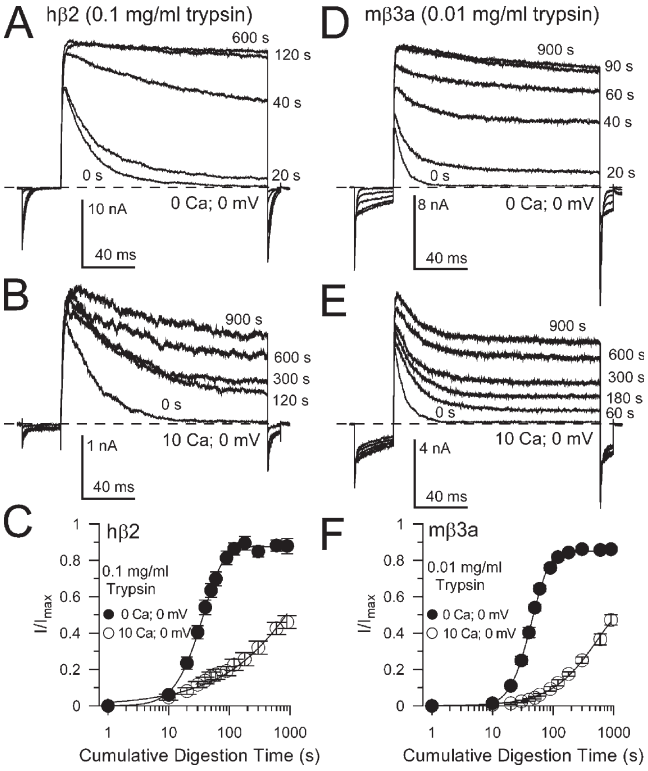

Figure 6. Digestion of mβ3a N termini is much faster than for β2. (A) Traces show removal of hβ2-mediated inactivation under closed-channel conditions (0 Ca^{2+}; 0 mV) with 0.1 mg/ml trypsin. (B) Traces show removal of β2-mediated inactivation by 0.1 mg/ml trypsin under inactivating conditions (10 μM Ca^{2+}; 0 mV). (C) The digestion time course is plotted for both closed (solid circles) and inactivating (open circles) hβ2 channels. (D) Sweeps monitor removal of mβ3a-mediated inactivation under closed-channel conditions, but with 0.01 mg/ml trypsin. Trypsin abolishes both the slow β3a tail currents and removes inactivation. (E) The time course of removal of mβ3a-mediated inactivation by 0.01 mg/ml trypsin is shown under inactivating conditions. Note that even at 900 s, appreciable inactivation still remains and that the slow β3a tail current persists. (F) The digestion time course for mβ3a channels is plotted for both closed-channel (solid circles) and inactivating (open circles) conditions.

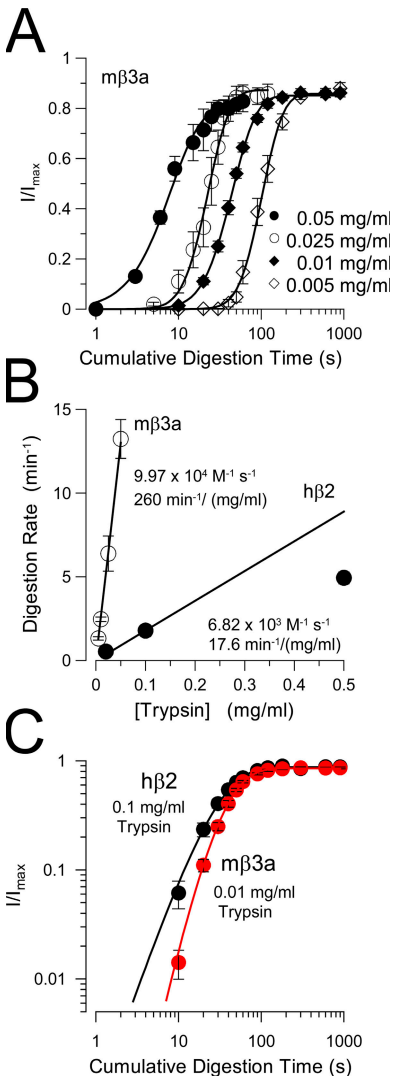

Figure 7. Comparison of removal of inactivation mediated by hβ2 and mβ3a. (A) The removal of mβ3a-mediated inactivation is plotted for four different trypsin concentrations. Fitted time constants of digestion were 5.83 ± 1.2 s (0.05 mg/ml), 10.5 ± 1.42 s (0.025 mg/ml), 23.72 ± 1.41 s (0.01 mg/ml), and 44.22 ± 3.74 s (0.005 mg/ml). (B) The effective digestion rate (min^{-1}) is plotted as a function of trypsin concentration for both mβ3a and hβ2 (from Zhang et al., 2006). The line through the mβ3a points corresponds to a linear fit with a slope of 260 min^{-1}/mg/ml, which assumes a molecular weight of 24 kD for trypsin corresponds to $9.97 \times 10^4\ M^{-1}\ s^{-1}$. For β2, the line corresponds to the slope through the two lowest trypsin concentrations, yielding a maximal effective rate of $6.82 \times 10^3\ M^{-1}\ s^{-1}$. (C) A log-log plot of the digestion time course for hβ2 (black circles) and mβ3a (red circles) compares the slope of the digestion process. For β2, $n = 2.21 \pm 0.23$; for β3a, $n = 3.62 \pm 0.39$. Note that in A, except for the time course observed with 0.05 mg/ml, the steeper slope of β3a digestion is independent of trypsin concentration. Similarly, the slope of β2 digestion is independent of trypsin concentration (not depicted).

Published February 23, 2009

retained in the N terminus (Fig. S4). When residue R16, R17, R18, or R21 was individually mutated to Q, the resulting constructs retained a sensitivity to 0.01 mg/ml trypsin that was only slightly less than wild-type mβ3a, with mutation of R18 and R21 having somewhat stronger effects than mutation of R16 and R17 (Fig. S4, A and B). However, when both R18 and R21 were mutated to Q, the resulting trypsin sensitivity was shifted ~10-fold (Fig. S4 C). We also examined constructs in which only a single basic residue was retained in the N terminus. In mβ3a-R16 and mβ3a-R17, 0.1 mg/ml trypsin removed inactivation with a time course similar to or slower than that of the effect of 0.01 mg/ml trypsin on wild-type mβ3a (Fig. S4 D). However, when only R21 (mβ3a-R21) was retained in the N terminus, 0.01 mg/ml trypsin removed inactivation with a time course only somewhat slower than for wild-type mβ3a (Fig. S3 E), whereas R18 (mβ3a-R18) more weakly supported digestion by 0.01 mg/ml trypsin. When a construct retained only R18 and R21 in the N terminus (mβ3a-R18 and -R21), digestion by 0.01 mg/ml trypsin was essentially indistinguishable from wild-type mβ3a (Fig. S4 F). These results indicate that R18 and R21 are probably the primary residues attacked by trypsin in the mβ3a N terminus, but, even in the absence of R18 and R21, both R16 and R17 will support digestion at rates comparable to the β2 N terminus.

These results show that two specific basic residues are largely responsible for wild-type mβ3a digestion rates. This is the same number of attackable basic residues as in the wild-type β2 N terminus, despite the fact that the mβ3a N terminus is digested at about a 10-fold faster rate than the β2 N terminus. We conclude that the number of digestible mβ3a basic residues is not the reason that the mβ3a N terminus is more rapidly digested.

Accounting for the Differences in Trypsin Digestion Rates of β3a and β2

The initial segments of both the β2 and β3a N termini are largely hydrophobic. We therefore examined the consequences of exchange or addition of these segments on each N terminus. In one case, we simply appended the first seven β2 residues FIWTSGR to the β3a N terminus to determine whether this might confer β2-like behavior on β3a. A related construct (FIWTSGQ) was also examined to remove the possible contribution of the β2 R8 arginine to the digestion process. Both FIWTSGR- β3a (Fig. 9 A) and FIWTSGQ- β3a (Fig. 9 B) exhibit sensitivity to digestion by 0.01 mg/ml trypsin, which is similar to wild-type β3a. Thus, the presence of the FIW motif, albeit at some distance from digestible β3a residues, has essentially no effect on the digestion rate. We also undertook a variety of other manipulations all using the addition of the FIW motif, but with other alterations in the β3a N terminus (Fig. S5). In all cases, trypsin removed inactivation with a time course more similar to that of wild-type mβ3a than of β2. Given the view that the FIW motif of the β2 N terminus binds within the antechamber, it seems likely that the FIW motif can also act similarly in at least some of these constructs. These results therefore suggest that the β3a N terminus, even when binding within the antechamber, may remain readily digestible by trypsin.

We then replaced the first 12 residues of the β2 N terminus with the first 12, largely hydrophobic residues of the β3a N terminus ($m\beta3a_{1\text{-}12}/\beta2_{13\text{-}end}$). This construct lacks the digestible R8 residue found in β2, and so therefore should be compared with mutated β2 constructs containing only the digestible R19 residue. This construct (Fig. 9 C) exhibited a sensitivity to 0.1 mg/ml trypsin (τ_d = 18.0 ± 0.90 ms) that was comparable to wild-type β2, but approximately two- to fourfold faster than digestion of β2 constructs containing only R19 (Zhang et al., 2006). Furthermore, $m\beta3a_{1\text{-}12}/\beta2_{13\text{-}end}$ exhibited a somewhat steeper digestion time course (n = 3.3 ± 0.3) reminiscent of β3a. The β3a N terminus

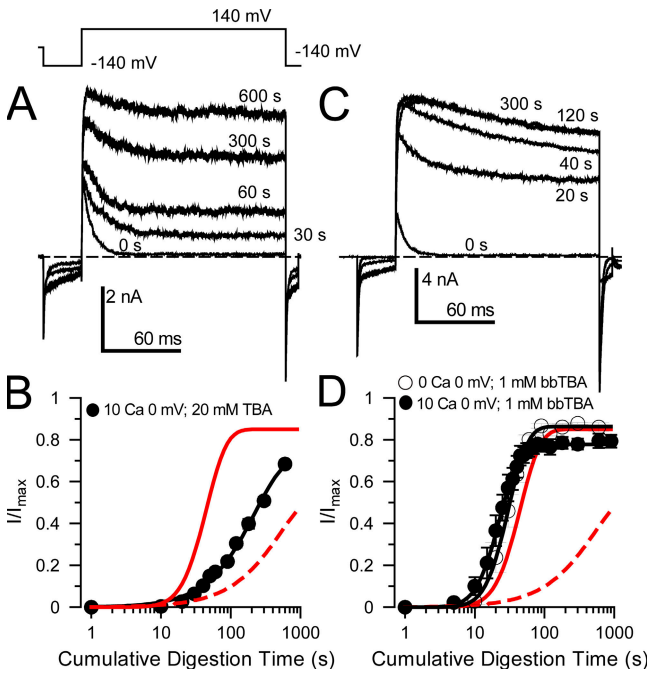

Figure 8. bbTBA and TBA differentially influence inactivation-associated protection against trypsin digestion for β3a subunits. (A) Traces show progressive removal by 0.01 mg/ml trypsin of inactivation mediated by β3a subunits with 20 mM TBA applied together with trypsin under inactivating conditions (10 μM Ca^{2+}; 0 mV). (B) The time course of the digestion process under inactivating conditions with TBA is compared with the normal time course of digestion of β3a under closed-channel (red line) or inactivated (dotted red line) conditions. (C) Traces show removal of inactivation when 0.01 mg/ml trypsin was applied along with 1 mM bbTBA under inactivating conditions. (D) Time course plots of removal of inactivation show that 1 mM bbTBA abolishes the protection normally produced by inactivation (dotted red line), but has little effect on the digestion time course (red line) under closed-channel conditions.

Published February 23, 2009

therefore partially substitutes for the FIW motif in constraining digestion of basic residues in the β2 N terminus, although perhaps binding somewhat more weakly within the antechamber.

If elements of both β3a and β2 N termini support antechamber binding, why are the two N termini digested at such apparently different rates and with such different power terms (n)? One possibility is that, although the hydrophobic part of both N termini may transiently bind within the antechamber, perhaps the segments containing the digestible basic residues (in β2, R8 and R19; in β3, R18 and R21) are not similarly accessible to trypsin when the N terminus is bound. Perhaps for the β2 N terminus, binding within the antechamber stabilizes a structure that is more resistant to digestion of the key basic residues than in a freely mobile N terminus. In contrast, for the β3a N terminus, perhaps the basic residues of bound β3a N termini retain sufficient flexibility to be indistinguishable from freely mobile N termini. To test the idea that the segments containing the basic residues might behave differently between the two N termini, segments containing previously identified trypsin-digestible basic residues were swapped between subunits. First, residues 12–21 from β3a replaced residues 14–22 in a β2 construct in which the 10 N-terminal basic residues were mutated to Q (β2-10$Q_{\Delta 14-22}$β3$a_{12\text{-}21}$). In this construct, trypsin-mediated digestion was slightly faster than wild-type β2 (Fig. 9 C), although clearly slower than for mβ3a. Similarly, a segment of β2 residues (14–22) was used to replace residues 13–21 in β3a (construct mβ3$a_{\Delta 13-21}$β$2_{14\text{-}22}$), such that the digestible R19 residue from β2 replaced the set of digestible residues in β3a. In this case (Fig. 9 D), removal of inactivation digestion with 0.1 mg/ml exhibited a complex time course perhaps best fit by two digestion components, one somewhat faster and one slower than for wild-type β2. Although we have no simple explanation for this behavior, compared with the digestion of wild-type β3a, the result suggests that replacement of the digestible segment of β3a with a segment from β2 does make the resulting construct somewhat less vulnerable to digestion by trypsin.

Although the above experiments fail to account fully for the difference in digestion rates of the two N termini, some conclusions can be drawn. First, the initial segment of the β3a N terminus does appear to substitute for the initial segment of the β2 N terminus in supporting inactivation and maintaining a digestion rate

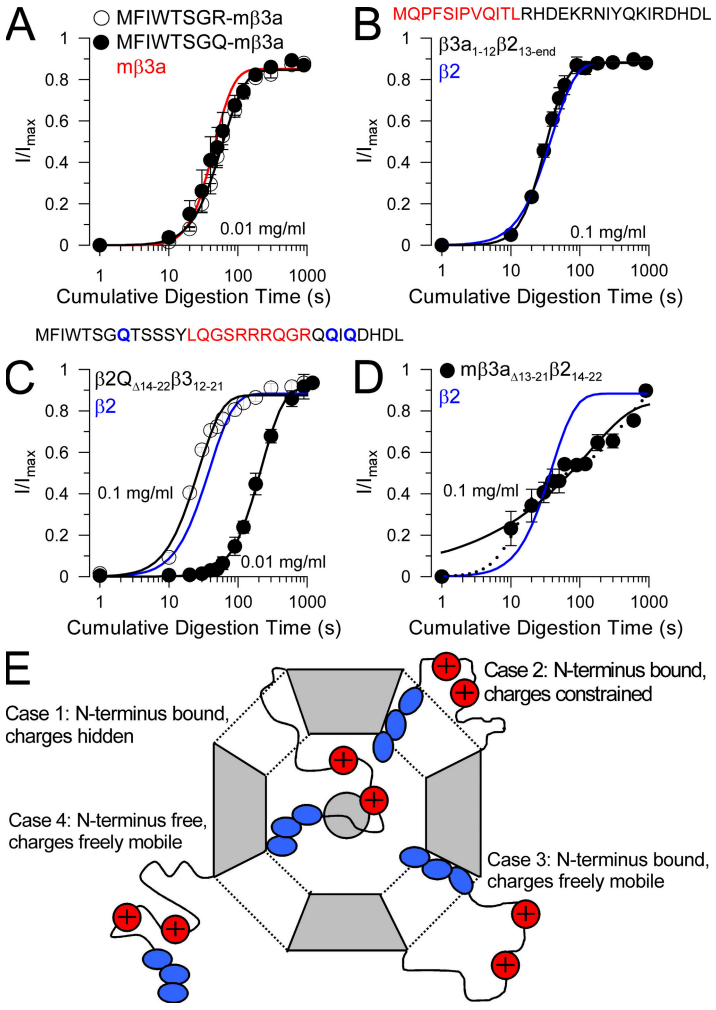

Figure 9. Exchange of hydrophobic and charged segments between β2 and hβ3a N termini. (A) The time courses of digestion under closed-channel conditions (0 Ca^{2+}; 0 mV) of the MFIWTSGR-β3a and MFIWTSGQ-β3a constructs are compared with wild-type mβ3a (red line) for 0.01 mg/ml trypsin. (B) The time course of digestion of β3$a_{1\text{-}12}$β$2_{13\text{-}end}$ (MQPFSIPVQITL from β3a appended to β2 at position 13) with 0.1 mg/ml trypsin is compared with the β2 digestion time course. (C) A β3a segment (residues 12–21 containing R16-18 and R21) replaced residues 14–22 in a β2 construct in which all N-terminal basic residues were replaced with Q. The plot shows the digestion time course for both 0.1 and 0.01 mg/ml trypsin compared with that of β2 (blue line). (D) The time course of digestion with 0.1 mg/ml trypsin of construct mβ3$a_{13\text{-}21}$β$2_{14\text{-}22}$ is compared with that of β2 (blue line). Dotted line represents a two-component exponential fit (analogous to Eq. 1) to the digestion time course, and the solid represents a fit of Eq. 1. (E) Possible configurations of N termini in a closed channel are schematized. Case 1, an N terminus is bound in the antechamber, and basic residues are shielded from digestion; Case 2, the N terminus is bound in the antechamber, but, although basic residues are outside the antechamber, they are structurally constrained, thereby hindering digestion; Case 3, the N terminus is bound in the antechamber, but basic residues are freely mobile and accessible to attack by trypsin; Case 4, an N terminus is freely mobile outside the antechamber allowing easy digestion by trypsin.

Published February 23, 2009

comparable to β2. This suggests that the β3a N terminus does bind within the antechamber, but perhaps with somewhat weaker affinity. Second, the digestible basic residues in the β2 N termini appear less readily digested than those of the β3a N terminus, although the addition of the β3a segment with basic residues produces only a slight increase in digestibility. The failure to observe a complete swap in properties may arise simply because of the limitations of the approach, in which a segment transferred from one N terminus to another may behave differently in the new background.

Within the context of Scheme 1, one might imagine that any given N terminus might adopt any of several possible configurations when channels are closed, each of which may differentially influence digestibility by trypsin. Fig. 9 E diagrams four possible situations. In Case 1, the binding of an N terminus within the antechamber may position basic residues within the antechamber, thereby effectively hiding the basic residues from attack by trypsin. In Case 2, when an N terminus is bound within the antechamber, it may constrain movement of the basic residues such that they are less vulnerable to attack by trypsin. In Case 3, when an N terminus is bound, the segment containing basic residues may reside outside the antechamber and be fully vulnerable to attack by trypsin. In Case 4, an unbound N terminus may be entirely outside the antechamber volume, with basic residues fully vulnerable to attack by trypsin within any constraints arising from any native N-terminal structure. For any N terminus in which the power term, *n*, for digestion is 2–3, the implication is that N termini that are bound within the antechamber are digested at slower rates than the freely mobile N termini outside the antechamber. However, the requirement of slower digestion is met by either Case 1 or Case 2, whereas Case 3 would be expected to produce little, if any, protection against trypsin digestion. mβ3a exhibits a faster digestion than β2 and contains the same number of digestible basic residues (two), and the mβ3a hydrophobic segment does appear to substitute with the FIW motif in supporting protection of digestion under closed-channel conditions for an otherwise β2 N terminus. Based on these differences, we propose that, under closed-channel conditions, the mβ3a N terminus behaves in a fashion similar to Case 3, whereas for β2 the N terminus behaves similarly to Case 2 (or perhaps Case 1). The failure of the $\beta3a_{12\text{-}21}$ segment to markedly increase β2 digestion may arise because the residual part of the β2 N terminus confers structural constraints on the β3a segment, thereby minimizing access of trypsin to this segment.

Protection under Closed-Channel Conditions May Arise because of Constraints on Motion of the N Terminus when Tethered at a Site within the Antechamber

Guided by the above models for N-terminal behavior in closed channels, we used a second approach to examine properties of protection against trypsin digestion under closed-channel conditions. In previous experiments, we examined the trypsin sensitivity of artificial N termini in which pairs of basic residues were positioned at different distances from an FIW inactivation segment (Zhang et al., 2006). These experiments showed that, when basic residues were <12 positions from the FIW motif, in inactivated channels those basic residues were in a position that could not be cleaved by trypsin. However, under closed-channel conditions, artificial N termini were digested at rates very comparable to digestion of β2 N termini under similar conditions. For the β2 N terminus, one might imagine that during binding within the antechamber some structure of the N terminus might preclude attack by trypsin even if the basic residues were outside the antechamber, but this explanation seems less likely for artificial N termini. Specifically, one might expect that artificial N termini would be sufficiently flexible that any basic residues positioned outside the antechamber under closed-channel conditions would be readily attacked by trypsin, therefore predicting a more rapid and steeper digestion time course than for the wild-type β2 N terminus. Yet, for an extensive set of artificial N termini (Zhang et al., 2006), the digestion of the artificial N termini exhibited power terms in the range of 1.5 to 2.5, with time constants comparable to the wild-type β2 N terminus. Because it seems likely that the basic residues for some of these constructs are outside the antechamber under closed-channel conditions, why are these power terms so low? Case 2 of Fig. 9 E would provide one possible explanation. For this to be the case, the poly-Q linkers used here must have structural constraints that reduce accessibility of trypsin to basic residues.

To further address this issue, we have created new artificial N termini in which basic residues are positioned either 8 residues (FIW-8Q-nK-20Q constructs) or 20 residues (FIW-20Q-nK-8Q constructs) from the FIW segment (Table I). Furthermore, we made versions of these constructs in which either two, three, or four basic residues were inserted. A variety of results seemed possible. If a 20Q spacer between basic residues and FIW is more likely to position the basic residues outside the antechamber, one might expect that the digestion rate under closed-channel conditions might be faster than in constructs with the 8Q spacer. If both 20Q and 8Q spacers position basic residues outside the antechamber, the closed-channel–associated digestion in both cases might be expected to be faster than for wild-type β2. Contrary to either of these expectations, the digestion time course was generally similar for constructs with either a 20Q or 8Q spacer (Fig. 10, A–C) regardless of whether there were two, three, or four basic residues on the N terminus. Furthermore, in all cases the digestion time course under closed-channel conditions was quite comparable to that of the wild-type β2 N terminus regardless of whether there were two, three, or four basic residues.

Published February 23, 2009

We think it is unlikely that this closed-channel protection can be explained by the idea that the basic residues in both the 8Q and 20Q constructs are positioned within the antechamber. If, on the contrary, the basic residues in the 20Q-xK-8Q constructs are positioned outside the antechamber, the persistent closed-channel protection might arise from contributions of the two factors mentioned above. First, when an N-terminal binding epitope binds within the antechamber, that binding may reduce the overall flexibility of the N terminus and, by minimizing the degrees of freedom of motion of that N terminus, reduce the likelihood of attack by trypsin. Second, the poly-Q linkers may adopt conformations that reduce accessibility of basic residues to attack by trypsin. Both of these explanations are consistent with Case 2 (Fig. 9 E). Overall, the results seem most consistent with the idea that protection under closed-channel conditions does not arise from the presence of the basic residues within the antechamber, but rather from structural constraints on the accessibility of trypsin to the digestible basic residues when an N terminus is bound within the antechamber.

If this hypothesis is correct, the digestion rate of an artificial N terminus under closed-channel conditions might be increased if the basic residues were embedded in a more flexible set of residues. We replaced the charged lysine residues in the artificial N termini with the m$\beta3a_{12\text{-}21}$ sequence (LQGGRRRQGR) containing the R16–R18 and R21 residues. In contrast to the digestion of FIW-20Q-KKK-8Q-β2, the FIW-20Q-$\beta3a_{12\text{-}21}$-8Q-β2 construct was found to be readily digested by 0.01 mg/ml trypsin (Fig. 10 D). This indicates that the intrinsic properties of the $\beta3a_{12\text{-}21}$ segment are probably an important determinant of the rapid digestion of the β3a N terminus compared with β2. Furthermore, the result suggests that the KKK residues in the FIW-20Q-KKK-8Q-β2 construct probably do reside outside the antechamber, but that such residues are somehow less accessible to digestion by trypsin than in a freely mobile N terminus. We also tested two mutated versions of the FIW-20Q-β3a12-21-8Q-β2 construct: one with R16Q/R17Q and the other with three G/Q substitutions. Both exhibited digestion rates comparable to β3a, suggesting that the R18R21 pair was sufficient to account for faster digestion, and that intrinsic flexibility conferred by glycine residues was not essential for the faster digestion.

We interpret these results as follows. Both β2 and β3a N termini likely bind in the antechamber, and segments

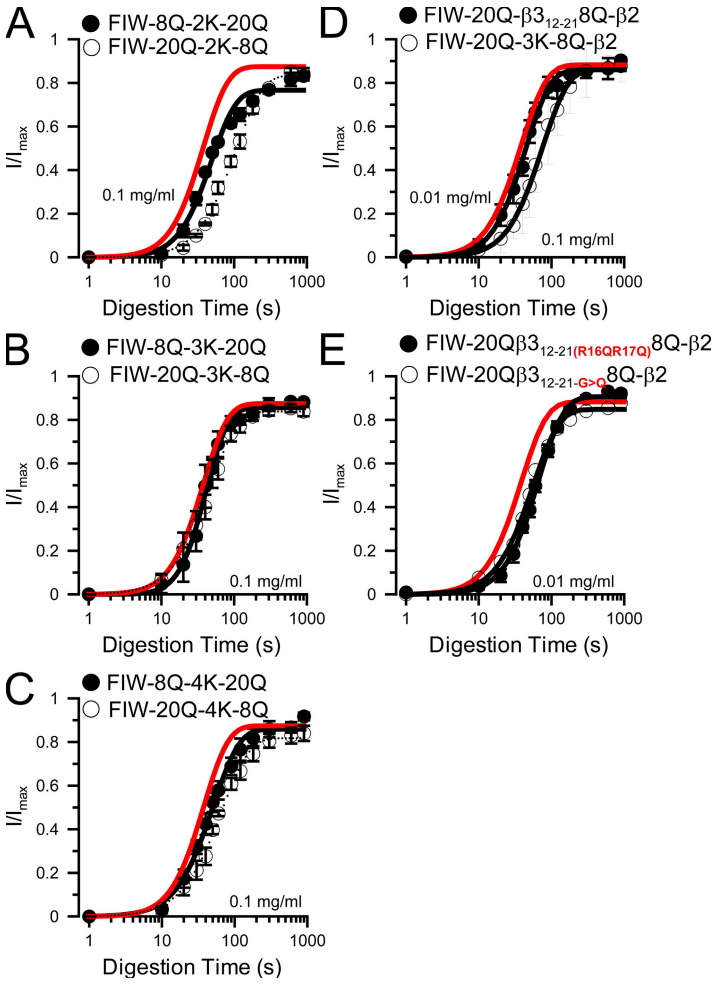

Figure 10. Impact of charge and the $\beta3a_{12\text{-}21}$ segment inserted in artificial N-terminal linkers on trypsin digestion rates under closed-channel conditions. (A) The time course of trypsin-mediated removal of inactivation (0.1 mg/ml trypsin) is compared for constructs FIW-8Q-2K-20Q-β2 and FIW-20Q-2K-8Q-β2, in which the N terminus length is identical, but the basic residues are positioned at either 8 or 20 residues from the FIW motif. The digestion time course of wild-type β2 is given by the red line. (B) The time courses of digestion for FIW-8Q-3K-20Q-β2 and FIW-20Q-3K-20Q-β2 are shown. (C) The time course of digestion for FIW-8Q-4K-20Q-β2 is compared with FIW-20Q-4K-8Q-β2. (D) The digestion time course with 0.01 mg/ml trypsin for a construct (FIW-20Q-$\beta3a_{12\text{-}21}$-8Q-β2) in which segment $\beta3a_{12\text{-}21}$ was inserted in an artificial N terminus is displayed (τ_d =28.9 ± 4.0 s; n = 2.3 ± 0.5) and compared with that of FIW-20Q-KKK-8Q with 0.1 mg/ml trypsin (τ_d = 52.5 ± 4.8 s; n = 2.0 ± 0.2 for a different set of patches than in B). (E) The time course of digestion by 0.01 mg/ml trypsin is shown for two constructs in which the $\beta3a_{12\text{-}21}$ segment (LQGGRRRQGR) contained additional substitutions. In one, R16Q and R17Q resulted in an N terminus in which only R18 and R21 remained (LQGGQQRQGR; τ_d = 45.4 ± 3.7 s; n = 2.1 ± 0.2). In the other, all glycines in the β3a segment were mutated to Q (τ_d = 40.3 ± 5.2 s; n = 1.8 ± 0.3).

Published February 23, 2009

containing potentially digestible basic residues are likely to be positioned outside the antechamber when the N terminus is bound. We propose that the differential closed-channel protection exhibited for different N termini arises because of differential flexibility of the tethered N termini. Specifically, when a β2 N terminus is bound in the antechamber, the digestible basic residues of the β2 N terminus and some artificial N termini are less digestible than in a freely mobile N terminus. In contrast, when a β3 N terminus is bound in the antechamber, the segment of digestible residues in the β3a N terminus retains sufficient flexibility to be digested at rates comparable to a freely mobile N terminus.

A Two-Site Protection Model Better Accounts for Some Aspects of Protection under Closed-Channel Conditions

The model given in Scheme 1 (Fig. 2 A) proposes that only a single N terminus can be protected by binding within the antechamber at a time. However, although values of $n < 4$ require that fewer than four N termini can be protected at a time, might two or three N termini be protected at a time rather than just one? In fact, one aspect of our results is at variance with the quantitative predictions of the one-site model. Namely, for a wild-type β2 construct that is digested with a power term of ~2.5, the one-site model predicts that, with complete removal of protection under closed-channel conditions ($n = 4$), the digestion τ_d should be faster by a factor of ~2–5 (Zhang et al., 2006). In contrast, for the W4G construct in which protection under closed-channel conditions is reduced (i.e., $n = \sim 3.4$), the digestion rate is about eightfold faster (Fig. 11). This suggests that, with complete removal of closed-channel–associated protection, the digestion process would be even faster, as was observed with β3a.

The estimated values of n represent the upper limit for the number of domains that must be protected. For protection mediated by inactivation, n approaches 1.0, consistent with the idea that high affinity binding of a single domain is involved. A value of n of 2.5 under closed-channel conditions argues that fewer than three, but possibly either one or two domains may be protected. Because most β2 constructs exhibit n values less than 3.0 but greater than 2.0, the possibility of a three-site protection model seems unlikely, but a two-site model must be considered. To evaluate this issue, we used a simplified form of Scheme 1 in which channels are assumed to be at low open probability with no

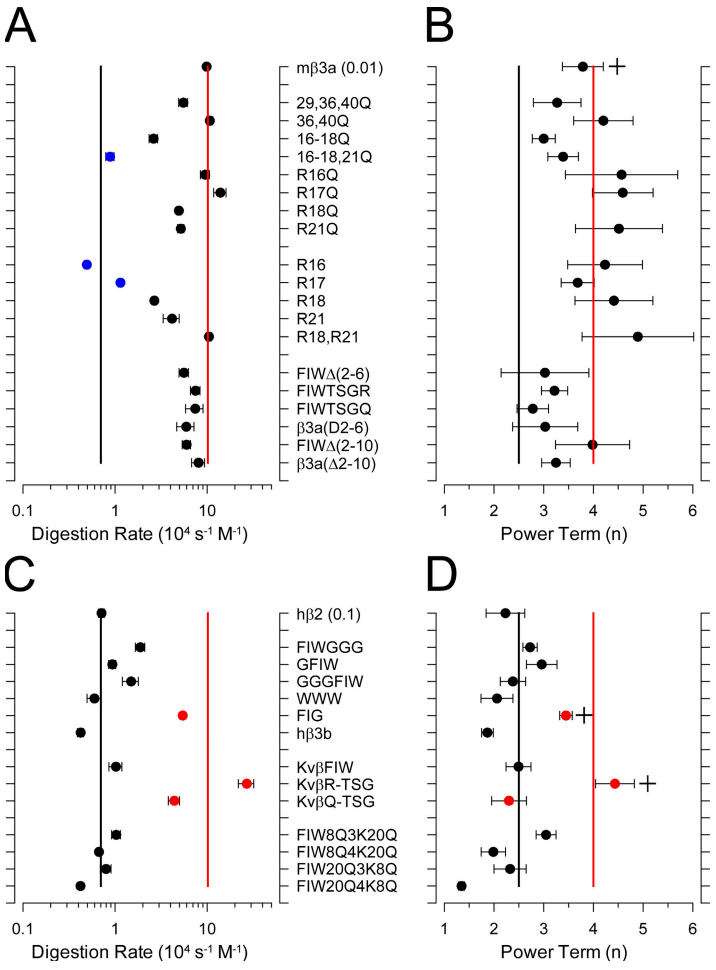

Figure 11. Summary of digestion rates and power terms for various constructs. (A) Apparent digestion rates were calculated for β3a-derived constructs. For the calculation of effect rates, the trypsin molecular weight was assumed to be 24 kD. Red line indicates rate measured for wild-type β3a, and the black line indicates the mean value for wild-type β2. Blue symbols indicate those constructs with the most strongly slowed digestion for β3a. (B) The fitted values for n are for β3a-derived constructs shown to cluster around $n = 4$. Although there seems to be a trend for FIW-tagged constructs to have a lower value of n, ANOVA comparisons of n from sets of patches revealed no statistically significant difference between β3a and any FIW-tagged construct. (C) Apparent digestion rates for β2-related constructs are plotted, with the three with the largest increase in digestion rate highlighted in red. (D) Power terms for β2 constructs cluster around $n = 2.5$. Values for FIG (W4G; P = 0.00542) and KvβTSGR (P = 7.01E-05) were found to be statistically different from wild-type β2 by ANOVA analysis, whereas comparison of n values for other constructs showed no difference with β2. Power terms for β2 and β3a were also significantly different (P = 0.00542).

Published February 23, 2009

inactivation (Fig. 12 A). Open and inactivated states are removed from the model with essentially no effect on the predicted time course of digestion under closed-channel conditions. We extended the single-site model in Scheme 1 to include the possibility that a second N terminus can also be protected from digestion by trypsin (Fig. 12 A). For both the one- and two-site formulations, we simulated the predicted digestion time course while varying the affinity of the protection site(s). This allowed determination of τ_d and n for different fractional occupancies of the protection sites (Fig. 12 B). For the one-site model, fractional occupancy of 1.0 corresponds to 100% occupancy of the single protection site by a single N terminus, whereas for the two-site model, fractional occupancy of 1.0 corresponds to 100% occupancy of two protection sites. Thus, for the one-site model, at high fractional occupancy, three N termini remain accessible to trypsin at most times, whereas for the two-site model, two N termini remain accessible. In both models, appreciable effects on digestion τ_d and n were predicted to occur only at fractional occupancies above ~0.75. The relationship between the predicted prolongation of τ_d and n (Fig. 12 C) for each model may provide a way to distinguish between them. For the one-site model, for n between 2 and 3, the digestion time constant is predicted to be only approximately two- to fivefold slower than that which would be observed when there is no closed-channel protection. In contrast, for the two-site model, for n between 2 and 3, the digestion τ_d is predicted to be ~5–20-fold slower than that expected for no closed-channel protection.

We observed that the W4G-β2 mutation exhibited a digestion rate (Figs. 3 and 11) that was approximately eightfold that of the wild-type β2 construct, whereas the power term, n, for W4G-β2 was ~3.4. With mutated β3a N termini containing only two digestible basic residues, the effective digestion rates were about almost 20-fold that of wild-type β2, with an n value close to 4.0. These results with W4G-β2 and β3a constructs set an upper limit on the potential increase in digestion rate that can occur in the absence of any closed-channel protection, and fold increase in rates is much greater than would be expected based on a strictly single-site protection model. Using the β3a digestion rate as that characteristic of an N terminus with two attackable basic residues, but with no closed-channel protection, we calculated the fold-prolongation for various mutated β2 N termini (as listed in Fig. 11). These prolongations relative to the fitted estimates of n, when compared (Fig. 12 C) to the

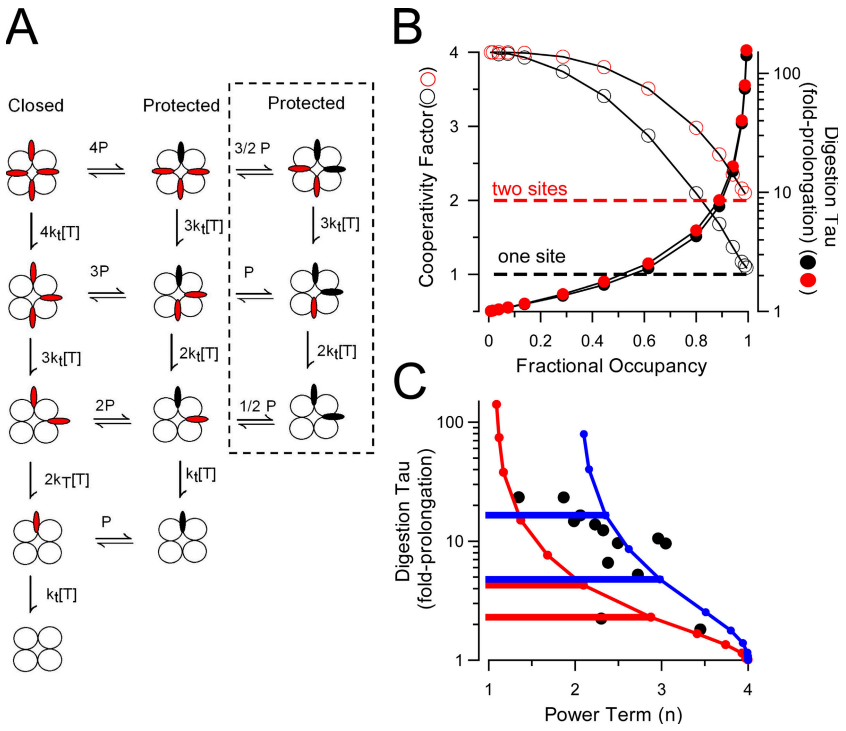

Figure 12. A model in which two N termini can dwell within the antechamber at a time may better account for the data. (A) The two left-hand columns of states correspond to Scheme 1 under conditions of low Po and no inactivation and, therefore, approximate closed-channel conditions for a model in which one N terminus can occupy the antechamber at a time. The additional states highlighted in the dotted rectangle propose that an additional N terminus can also bind, presumably in the antechamber, thereby being protected from digestion by trypsin. Red and black ovoids correspond to unprotected and protected N termini, respectively. (B) Both one- and two-site models were used to simulate the trypsin-mediated removal of inactivation over a range of values of P, the binding constant for the site producing closed-channel–associated protection. Fractional occupancy was calculated as: $P_a = p_f/(p_f+p_r)$, where p_f and p_r are defined as the rates of binding and unbinding of an N terminus in the antechamber (Table II). Both models predict a similar prolongation of τ_d (filled circles) with occupancy within the antechamber, whereas the two differ in regards to the limiting power term at high fractional occupancies (open circles). Note that, for the one-site model, the relationship between fractional occupancy, prolongation of τ_d, and n were plotted incorrectly in our previous report (Zhang et al., 2006), as described in Materials and methods. (C) The prolongation of τ_d is plotted as a function of the power term for the one-site (red) and two-site (blue) models. The horizontal lines mark the range of prolongations, relative to the case for $n = 4$, expected for power terms in the range of 2 to 3. The filled black circles correspond to measurements of n and calculations of prolongation of τ_d for wild-type β2 and mutated β2 constructs, assuming that the digestion rate of β3a most closely reflects digestion of an N terminus without protection in the antechamber. If the rate of digestion of the W4G construct is used as the τ_d(min), the points are shifted leftward, but still favor the idea that two sites are involved in closed-channel–associated protection.

Published February 23, 2009

predictions of the one- and two-site models, suggest that a two-site model may better account for the experimentally observed range of values for τ_d and n.

DISCUSSION

Several ion channels contain cytosolic domains that are appended to the membrane-embedded, pore-forming domains and play important roles in regulation of channel gating (Gulbis et al., 2000; Schumacher et al., 2001; Jiang et al., 2002; Xia et al., 2004). Both for Kv channels (Gulbis et al., 2000; Kobertz et al., 2000) and for BK channels (Zhang et al., 2006), it has been proposed that, because of the appended cytosolic structure "hanging" from the pore-forming domain, mobile cytosolic inactivation domains access their positions of inactivation laterally by passing through side portals between the membrane and cytosolic domains (e.g., Fig. 1 A). Our previous study had proposed that, under closed-channel conditions and even more so under inactivating conditions, β2 N termini were protected from digestion by trypsin (Zhang et al., 2006). These observations led to a model in which inactivation domains could be protected from trypsin digestion by occupancy within a protected volume between the pore domain and cytosolic domain. The specific lengths of artificial N termini that were either unprotected or protected from trypsin digestion during inactivation also allowed some suggestions regarding the dimensions of the protected space.

Here, we have evaluated several predictions of this model to define more clearly whether protection of N termini occurs under conditions in which channels are predominantly closed, what the stoichiometry of that protection may be, and whether these properties are generalizable to a variety of different N termini. The results included three observations that provide strong support for the idea that, under closed-channel conditions, β2 N termini can be protected from trypsin digestion, and that the sites involved in closed-channel–associated protection are distinct from the site involved in inactivation-associated protection against digestion. First, closed-channel–associated protection predicts that reduction of affinity of the N termini for the antechamber site of protection will speed up digestion. This was observed in some constructs. Second, the proposal predicts that disruption of closed-channel–associated protection will result in a steeper power term in the digestion time course. This is also observed with particular constructs. Third, the idea that closed-channel–associated protection and inactivation-associated protection involve distinct sites of binding of a β subunit N terminus was supported by two observations: first, that bbTBA disrupted inactivation-associated protection but not closed-channel–associated protection, and, second, that different N-terminal constructs had differential effects on closed-channel–associated protection compared with inactivation-associated protection. On balance, then, the results provide strong support for the general model outlined at the outset. Finally, analysis of the variation of digestion τ_d with estimates of n allowed the proposal that protection against digestion under closed-channel conditions may involve similar binding of up to two N-terminal domains.

A key element in the argument that, under closed-channel conditions, N termini can be protected from digestion by trypsin was the observation that the power term, n, in fits of Eq. 1 to the digestion time course exhibited values in the range of 2.0 to 3.0 (Zhang et al., 2006). This required a model in which N termini are not equally digestible at all times by trypsin, and we have shown that the power term, n, can approach 4 with manipulations that might be expected to disrupt closed-channel–associated protection. Because the digestion time course is defined by a rather limited set of time points, we have been concerned about the robustness of the estimates of n. However, several factors provide confidence that the differences in n reported here do reflect underlying differences in the protection mechanism. First, for cases in which a β2 N terminus is made more readily digestible, an increase in n is also observed. However, simply changing the β2 digestion rate by varying [trypsin] has no effect on estimates of n (Zhang et al., 2006). Second, for hβ3a for which closed-channel–associated protection does not appear to occur and the power term approaches 3.6, slowing digestion by removing key basic residues does not alter the power term (Fig. 11 and Figs. S1 and S2). Thus, values of n approaching 4 are consistently observed for β3a-derived constructs. Third, the differences among estimates of n between pairs of constructs showed statistically significant differences (Fig. 11), e.g., between β2 and β2-W4G. These considerations provide confidence that the estimates of n are indicative of the properties of closed-channel–associated protection for a given construct.

What Is the Mechanistic Basis for Closed-Channel–associated Protection?

The simple fact that the stoichiometry for closed-channel–associated protection is <4 requires that binding by some N termini excludes other N termini from simultaneously occupying a similar site. For a one-site antechamber model, we had supposed that the basic physical dimensions of the β2 N terminus and likely dimensions of the channel antechamber (e.g., Fig. 1 A) might prevent other N termini from a similar position of protection (Zhang et al., 2006). There is no information concerning how much of the antechamber might be occupied by an individual N terminus when it is in a position of protection and, in fact, our results seem more consistent with the idea that two N termini may simultaneously occupy positions of protection within the antechamber while excluding access of the other

Published February 23, 2009

two N termini to similar positions. Given the limited dimensions of the antechamber and the size of the β2 N terminus (Jiang et al., 2002; Zhang et al., 2006), the idea that only one or two N termini may occupy this space at a time seems plausible. It is unlikely that this binding is somewhere besides the antechamber, because the simplest way of achieving a stoichiometry of <4 requires competition for sites accessible to all N termini. It should also be realized that the observed stoichiometry arises not because there are two antechamber binding sites, but rather because once two sites are occupied, no more N termini can reach any other sites.

Once an N terminus binds within the antechamber in a closed channel, how does this reduce digestion by trypsin? We considered four possible N-terminal configurations that might impact on digestion (Fig. 9 E). The most basic protection mechanism would be that, when an N terminus is bound within the antechamber, digestible basic residues are also within the antechamber (Fig. 9 E, Case 1). This mechanism likely applies to inactivation-associated protection because in artificial N termini, basic residues within 11 positions of the terminal FIW epitope are protected from digestion, whereas positions >11 amino acids from the FIW abolish inactivation-associated protection (Zhang et al., 2006). However, for closed-channel–associated protection, we do not know whether the digestible residues in either β2 or β3a are completely hidden within the antechamber when the N terminus is bound. As illustrated by Case 2 (Fig. 9 E), when an N terminus is bound, it may be that the flexibility and motion in the linker are restricted or a secondary structure is enforced, such that even if the basic residues are not within the antechamber, they may not be readily digestible by trypsin. In contrast, for other N termini, binding in the antechamber may fail to place structural constraints on the digestible basic residues (Fig. 9 E, Case 3), such that protection in closed channels does not occur. Finally, some N termini may fail to bind appreciably in the antechamber (Fig. 9 E, Case 4).

Through the swapping of segments between β2 and β3 N termini and examination of the properties of digestion of artificial N termini, our results favor the view that, when N termini are protected from digestion under closed-channel conditions, digestible basic residues are unlikely to be hidden within the antechamber itself. Rather, we propose that the faster digestion of the β3a N terminus compared with β2 arises because the segment containing the digestible R18 and R21 residues in β3a exhibits marked flexibility, even when the hydrophobic end of the β3a N terminus is bound in the antechamber. This flexibility around the basic residues (Case 3) thereby permits digestion by trypsin in a fashion similar to an N terminus entirely outside the antechamber (Case 4). In contrast, we propose that the β2 N terminus, when bound in the antechamber, places constraints on the R8 and R19 β2 residues, making them less accessible to digestion by trypsin than if the N terminus is freely mobile.

This view that different N termini, when bound in the antechamber, may have different rates of digestion because of flexibility of the region around the basic residues may also explain results with artificial β2 N-terminal linkers. Specifically, to explain the similarity of digestion rates of artificial β2 N termini and wild-type β2, we propose that, when the FIW motif is tethered to a site within the antechamber, the mobility of the linker in the artificial N terminus is sufficiently constrained in motion so that it provides some protection against attack by trypsin. This idea was given further support by the demonstration that insertion of the β3a segment of basic residues into an artificial N terminus resulted in digestion rates more comparable to β3a than β2, suggesting that this particular β3a segment has more flexibility that the lysine residues embedded in the polyglutamine chain. This idea that the polyglutamine N termini may confer some constraint on accessibility of trypsin to the basic residues seems surprising given that several studies suggest that polyglutamine chains are largely random coils (Wang et al., 2006; Vitalis et al., 2007), only transiently adopting shorter, more ordered features (Leitgeb et al., 2007). Intrinsically, we would have expected that such chains should not adopt structures that might preclude attack by trypsin on basic residues. However, our observations here clearly raise the possibility that the polyglutamine chains we have used may not behave like random coils or may at least transiently adopt some sort of constrained structure that makes them less amenable to attack than the native β3a N terminus. Potentially, the method used here could be exploited to undertake a quantitative examination of chain flexibilities of different composition, with a variety of consensus substrate sequences.

Summary

The results here support a model in which β2 and β3a N-terminal inactivation domains can transiently bind to sites that confer protection against digestion by trypsin. Two types of protection can occur. When an N terminus produces inactivation, that N terminus appears to be absolutely protected from digestion by trypsin. However, in closed channels, N termini can also transiently bind to a site distinct from the site involved in inactivation-associated protection. The data are most consistent with the idea that up to two N termini can be simultaneously protected from digestion by trypsin. Because protection in closed channels involves fewer than four N termini, the site of binding of the N terminus is most likely within the antechamber of the channel. The protection against digestion by trypsin that occurs in closed channels appears to arise, not because the basic residues are shielded within the antechamber, but rather because basic residues in the bound N terminus are less accessible to trypsin digestion than basic residues in a freely mobile N terminus.

We thank Yefei Cai for injection and care of oocytes.

This work was supported by National Institutes of Health grant GM081748 to C.J. Lingle.

Edward N. Pugh Jr. served as editor.

Submitted: 14 July 2008
Accepted: 3 February 2009

REFERENCES

Benzinger, G.R., X.M. Xia, and C.J. Lingle. 2006. Direct observation of a preinactivated, open state in BK channels with β2 subunits. *J. Gen. Physiol.* 127:119–131.

Ding, J.P., Z.W. Li, and C.J. Lingle. 1998. Inactivating BK channels in rat chromaffin cells may arise from heteromultimeric assembly of distinct inactivation-competent and noninactivating subunits. *Biophys. J.* 74:268–289.

Gulbis, J.M., M. Zhou, S. Mann, and R. MacKinnon. 2000. Structure of the cytoplasmic beta subunit-T1 assembly of voltage-dependent K^+ channels. *Science.* 289:123–127.

Hamill, O.P., A. Marty, E. Neher, B. Sakmann, and F.J. Sigworth. 1981. Improved patch-clamp techniques for high-resolution current recording from cells and cell-free membrane patches. *Pflugers Arch.* 391:85–100.

Jiang, Y., A. Lee, J. Chen, M. Cadene, B.T. Chait, and R. MacKinnon. 2002. Crystal structure and mechanism of a calcium-gated potassium channel. *Nature.* 417:515–522.

Kobertz, W.R., C. Williams, and C. Miller. 2000. Hanging gondola structure of the T1 domain in a voltage-gated K^+ channel. *Biochemistry.* 39:10347–10352.

Leitgeb, B., A. Kerenyi, F. Bogar, G. Paragi, B. Penke, and G. Rakhely. 2007. Studying the structural properties of polyalanine and polyglutamine peptides. *J. Mol. Model.* 13:1141–1150.

Li, W., and R.W. Aldrich. 2004. Unique inner pore properties of BK channels revealed by quaternary ammonium block. *J. Gen. Physiol.* 124:43–57.

Lingle, C.J., X.-H. Zeng, J.-P. Ding, and X.-M. Xia. 2001. Inactivation of BK channels mediated by the N-terminus of the β3b auxiliary subunit involves a two-step mechanism: possible separation of binding and blockade. *J. Gen. Physiol.* 117:583–605.

Schumacher, M.A., A.F. Rivard, H.P. Bachinger, and J.P. Adelman. 2001. Structure of the gating domain of a Ca^{2+}-activated K^+ channel complexed with Ca^{2+}/calmodulin. *Nature.* 410:1120–1124.

Solaro, C.R., J.P. Ding, Z.W. Li, and C.J. Lingle. 1997. The cytosolic inactivation domains of BK_i channels in rat chromaffin cells do not behave like simple, open-channel blockers. *Biophys. J.* 73:819–830.

Uebele, V.N., A. Lagrutta, T. Wade, D.J. Figueroa, Y. Liu, E. McKenna, C.P. Austin, P.B. Bennett, and R. Swanson. 2000. Cloning and functional expression of two families of beta-subunits of the large conductance calcium-activated K^+ channel. *J. Biol. Chem.* 275:23211–23218.

Vitalis, A., X. Wang, and R.V. Pappu. 2007. Quantitative characterization of intrinsic disorder in polyglutamine: insights from analysis based on polymer theories. *Biophys. J.* 93:1923–1937.

Wallner, M., P. Meera, and L. Toro. 1999. Molecular basis of fast inactivation in voltage and Ca^{2+}-activated K^+ channels: a transmembrane beta-subunit homolog. *Proc. Natl. Acad. Sci. USA.* 96:4137–4142.

Wang, X., A. Vitalis, M.A. Wyczalkowski, and R.V. Pappu. 2006. Characterizing the conformational ensemble of monomeric polyglutamine. *Proteins.* 63:297–311.

Wang, Y.-W., J.P. Ding, X.-M. Xia, and C.J. Lingle. 2002. Consequences of the stoichiometry of *Slo1* α and auxiliary β subunits on functional properties of BK-type Ca^{2+}-activated K^+ channels. *J. Neurosci.* 22:1550–1561.

Wilkens, C.M., and R.W. Aldrich. 2006. State-independent block of BK channels by an intracellular quaternary ammonium. *J. Gen. Physiol.* 128:347–364.

Xia, X.-M., J.P. Ding, and C.J. Lingle. 1999. Molecular basis for the inactivation of Ca^{2+}- and voltage-dependent BK channels in adrenal chromaffin cells and rat insulinoma tumor cells. *J. Neurosci.* 19:5255–5264.

Xia, X.-M., J.-P. Ding, X.-H. Zeng, K.-L. Duan, and C.J. Lingle. 2000. Rectification and rapid activation at low Ca^{2+} of Ca^{2+}-activated, voltage-dependent BK currents: consequences of rapid inactivation by a novel β subunit. *J. Neurosci.* 20:4890–4903.

Xia, X.-M., X.-H. Zeng, and C.J. Lingle. 2002. Multiple regulatory sites in large-conductance calcium-activated potassium channels. *Nature.* 418:880–884.

Xia, X.-M., J.P. Ding, and C.J. Lingle. 2003. Inactivation of BK channels by the NH_2 terminus of the β2 auxiliary subunit: an essential role of a terminal peptide segment of three hydrophobic residues. *J. Gen. Physiol.* 121:125–148.

Xia, X.-M., X. Zhang, and C.J. Lingle. 2004. Ligand-dependent activation of Slo family channels is defined by interchangeable cytosolic domains. *J. Neurosci.* 24:5585–5591.

Zeng, X., X.M. Xia, and C.J. Lingle. 2008. Species-specific differences among KCNMB3 BK β3 auxiliary subunits: some β3 variants may be primate-specific subunits. *J. Gen. Physiol.* 132:115–129.

Zhang, Z., Y. Zhou, J.P. Ding, X.M. Xia, and C.J. Lingle. 2006. A limited access compartment between the pore domain and cytosolic domain of the BK channel. *J. Neurosci.* 26:11833–11843.

Zhou, M., J.H. Morais-Cabral, S. Mann, and R. MacKinnon. 2001. Potassium channel receptor site for the inactivation gate and quaternary amine inhibitors. *Nature.* 411:657–661.

Zhang et al., http://www.jgp.org/cgi/content/full/jgp.200810079/DC1

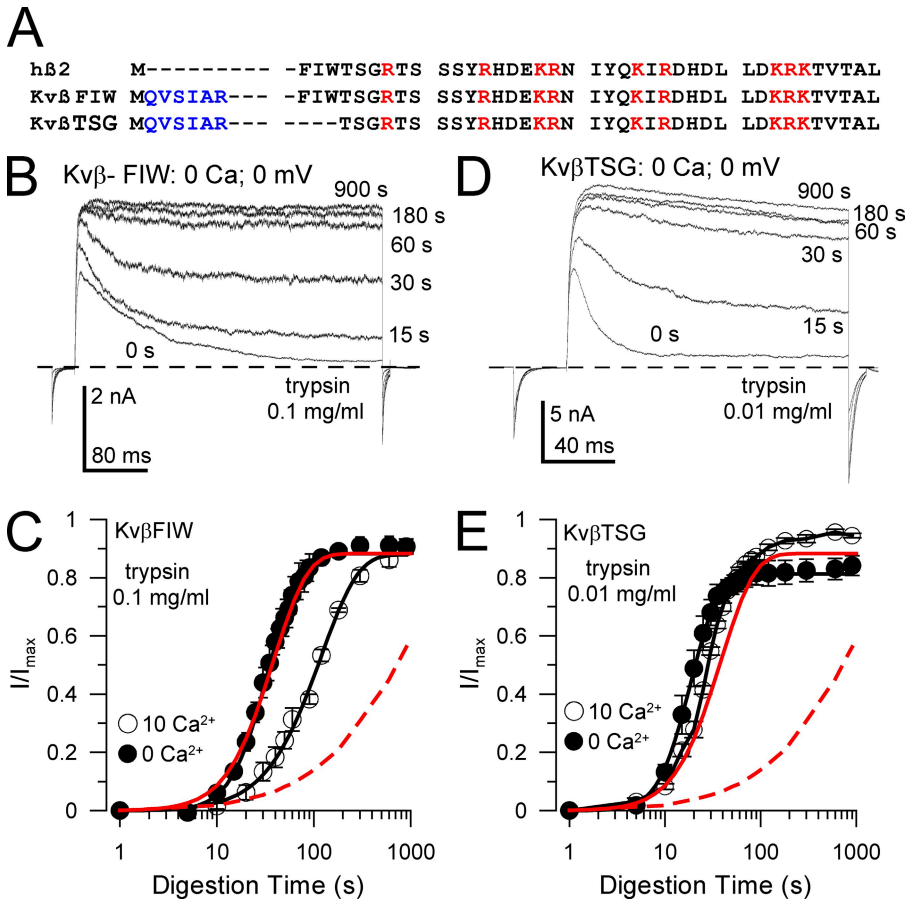

Figure S1. Replacement of the β2 FIW motif with a Kv inactivation segment also speeds up the closed channel–associated digestion rate. (A) Sequences show wild-type β2 along with constructs in which the first six residues from the Kvβ1.2 inactivation segment were added just before the β2 FIW motif (KvβFIW) or replaced the FIW motif (KvβTSG). (B) Test traces for KvβFIW are shown during digestion by 0.1 mg/ml trypsin under closed-channel conditions (0 Ca^{2+}; 0 mV). (C) The time course of digestion for KvβFIW for closed-channel (open circles) and inactivating (filled circles) conditions are shown along with red lines showing the trypsin digestion time course of wild-type β2 N termini. Appending the Kvβ motif reduces the protection due to inactivation, but has little effect on closed channel–associated digestion. (D) Test traces for KvβTSG during digestion by 0.01 mg/ml trypsin at 0 Ca^{2+}, 0 mV are shown. (E) The digestion time courses with 0.01 mg/ml trypsin for KvβTSG under closed-channel and inactivating conditions are plotted, along with the time course for digestion of β2 with 0.1 mg/ml trypsin. Note the steeper digestion time course for the KVβTSG construct.

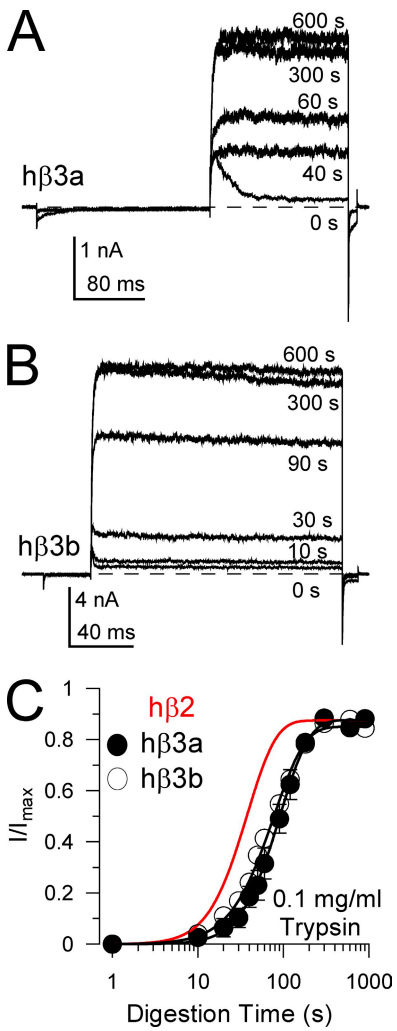

Figure S2. Human β3a and β3b N termini are digested at rates similar to the β2 N terminus. (A) Traces show removal of inactivation mediated by the human β3a subunit with 0.1 mg/ml trypsin. The slower digestion of the hβ3a N terminus compared with mouse β3a is proposed to arise from the residual inactivation mediated by the portion of the human β3 N terminus that persists after rapid digestion by trypsin of basic residues in the initial β3a-specific N-terminal–specific segment. (B) Traces show removal of inactivation mediated by the human β3b subunit with 0.1 mg/ml trypsin. (C) The time courses of digestion of both hβ3a (filled circles) and hβ3b (open circles) by 0.1 mg/ml trypsin are compared with the time course for digestion of human β2 (red line). These results are rationalized as follows. In mouse, a putative β3b′ N terminus does not produce inactivation, primarily because the mouse N terminus is six residues shorter and has fewer hydrophobic residues (Zeng, X., X.M. Xia, and C.J. Lingle. 2008. *J. Gen. Physiol.* 132:115–129). Therefore, in both human and mouse β3a, rapid digestion of R18 and R21 leaves a residual N terminus that is similar to the corresponding β3b. In mouse, the residual N terminus is not competent to produce any residual inactivation, so only the rapid β3a digestion is monitored. However, in hβ3a, cleavage of R18-R21 results in a residual inactivation-competent N terminus that is digested at the slow rates characteristic of hβ3b. The traces evoked by test pulses to +80 mV during digestion of hβ3b show that, within 40 s of trypsin application, the slow tail characteristic of β3a action is entirely removed, although the steady-state current continues to increase over several hundred seconds.

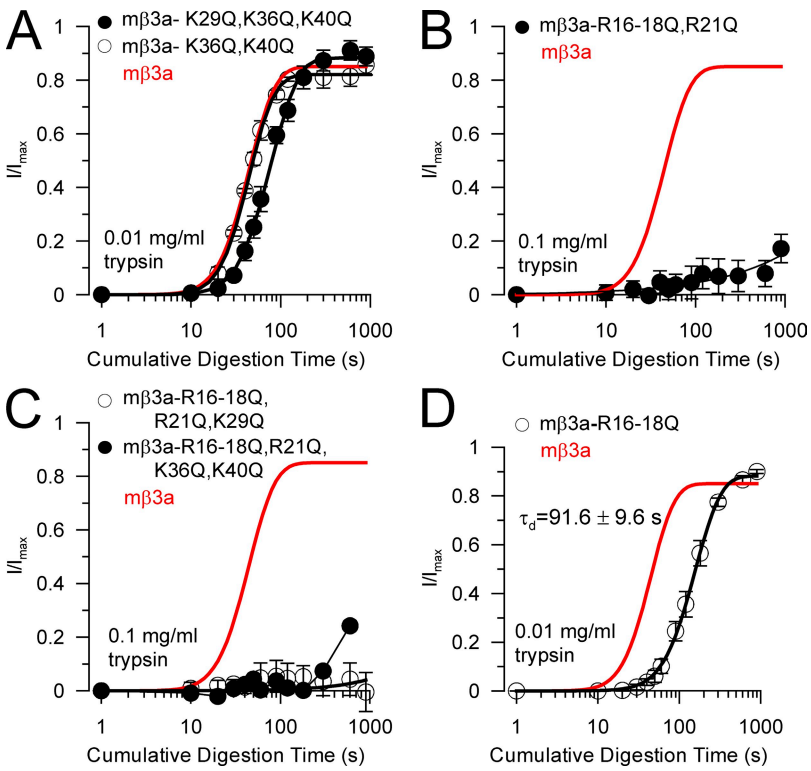

Figure S3. Residues K29, K36, and K40 do not contribute to β3a trypsin sensitivity, but R16, R17, R18, and R21. (A) The time course of removal of inactivation by 0.01 mg/ml trypsin is shown for constructs in which K36 and R40 were neutralized to Q, or K29, K36, and K40 were neutralized to Q. In both cases, the digestion time course is similar to that of wild-type β3a (red line). (B) 0.1 mg/ml trypsin has little ability to remove inactivation in a construct in which residues R16, R17, R18, and R21 were replaced with Q. (C) 0.1 mg/ml trypsin has little affect on constructs in which either R16, R17, R18, R21, and K29 were replaced with Q or when R16, R17, R18, R21, K36, and K40 were replaced with Q. (D) When R16, R17, and R18 were replaced by Q, the resulting construct was digested approximately three- to fourfold slower than wild-type β3a (red line), suggesting that R21 is sufficient to support digestion.

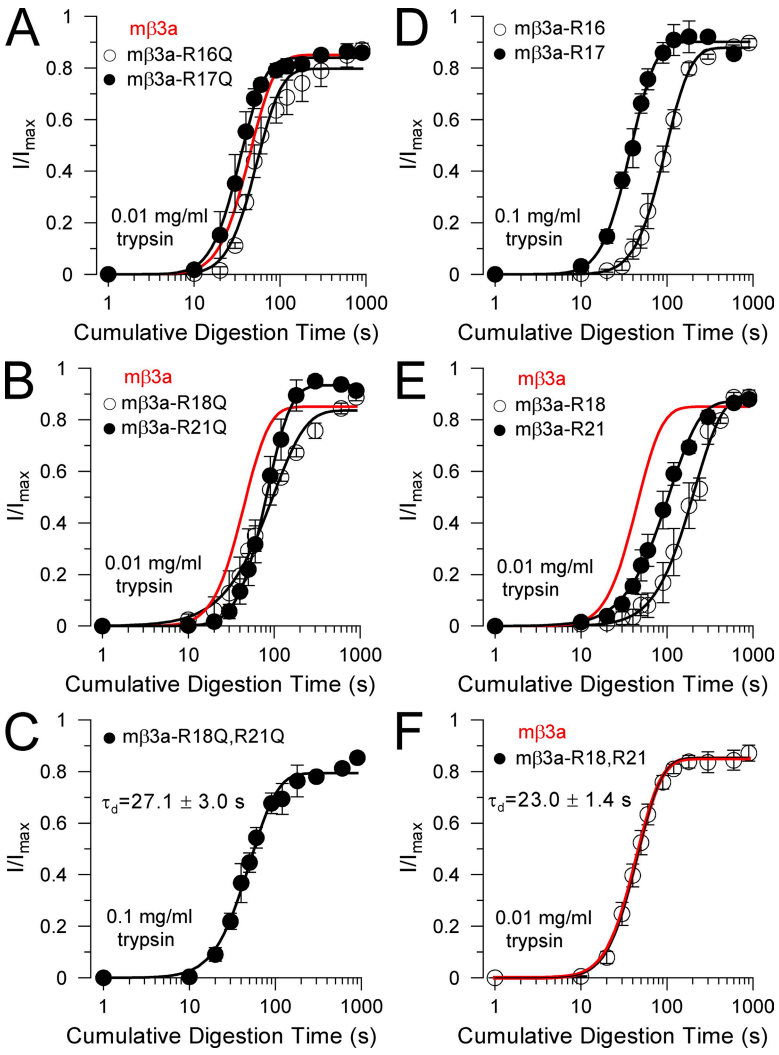

Figure S4. Residues R18 and R21 appear to be the main determinants of trypsin sensitivity of the β3a N terminus, but R16 and R17 also can contribute. (A) β3a-R16Q and β3a-R17Q are digested by 0.01 mg/ml trypsin with a time course similar to that of wild-type β3a (red line). (B) β3-R18Q and β3a-R21Q are digested by 0.01 mg/ml trypsin only somewhat more slowly than wild-type β3a. (C) β3a-R18Q,R21Q is digested by 0.1 mg/ml trypsin with a time course similar to β2, suggesting an ∼10-fold weaker sensitivity to trypsin than wild-type β3a. (D) Trypsin sensitivity is shown for two constructs, mβ3a-R16 and mβ3a-R17, in which all basic residues were neutralized to Q, except R16 and R17, respectively. These single basic residues were sufficient to support appreciable digestion by 0.1 mg/ml trypsin, but at rates comparable to or slower than wild-type β2. (E) When only R18 (mβ3a-R18) or R21 (mβ3a-R21) were the sole basic residues in the N terminus, 0.01 mg/ml trypsin was able to support appreciable removal of inactivation, albeit at rates somewhat slower than wild-type β3a. (F) In the mβ3a-R18,R21 construct, R18 and R21 were the only remaining basic residues. In this case, digestion by 0.01 mg/ml trypsin was indistinguishable from digestion of wild-type β3a.

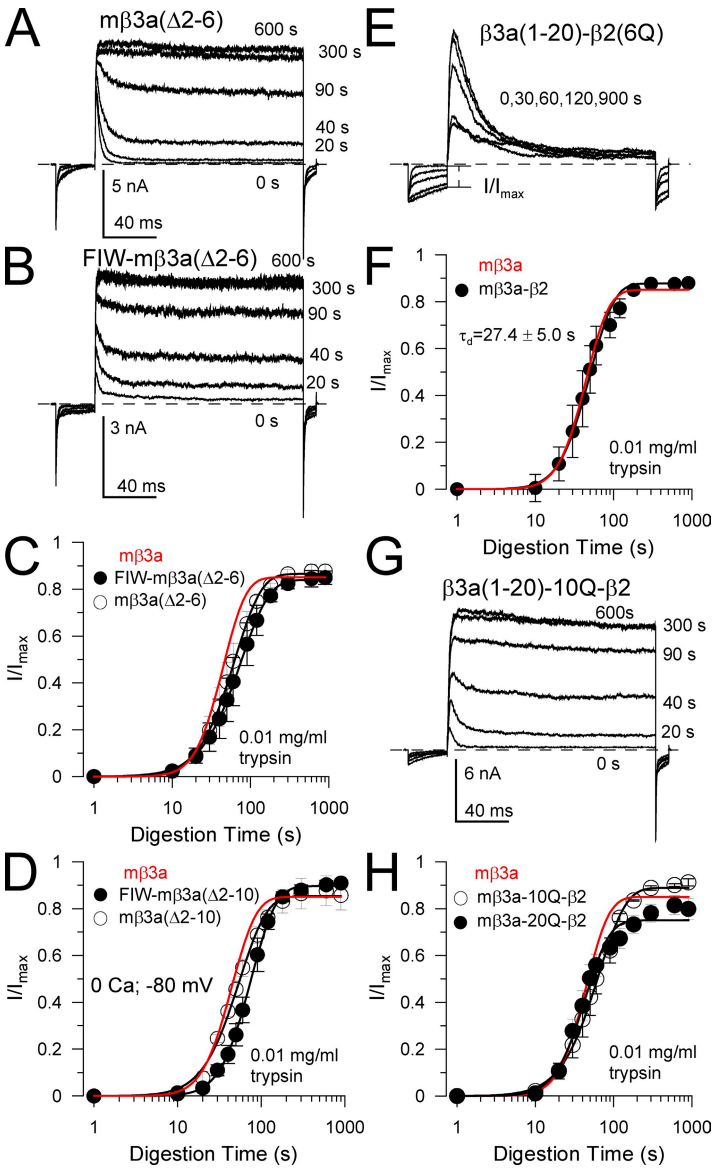

Figure S5. Manipulations of the β3a N terminus are unable to slow trypsin-mediated digestion of β3a. (A) Traces show removal of inactivation mediated by an mβ3a N terminus in which residues two to six were deleted with 0.01 mg/ml trypsin. (B) Traces show removal of inactivation (with 0.01 mg/ml trypsin) mediated by a construct in which the β2 hydrophobic motif, FIW, replaced residues two to six in the β3a N terminus. (C) The time course of trypsin-mediated removal of inactivation is plotted for both mβ3a(Δ2-6) and FIW-mβ3a(Δ2-6), showing little difference compared with wild-type mβ3a (red line). (D) The time course of removal of inactivation is plotted for both m β3a (Δ2-10) and FIW-mβ3a(Δ2-10) constructs, again showing little difference with wild-type mouse β3a. (E) Traces show currents activated at different times of digestion (by 0.01 mg/ml trypsin) in a construct in which the first 20 residues of β3a were appended to the beginning of a β2 construct in which the first six basic residues were neutralized to Q. Neutralization of such residues completing abolishes trypsin sensitivity of β2 (Zhang, Z., Y. Zhou, J.P. Ding, X.M. Xia, and C.J. Lingle. 2006. *J. Neurosci.* 26:11833–11843). Digestion of the β3a basic residues results in larger inactivating currents, but inactivation is retained because of the presence of the residual inactivating β2 N terminus. With an intact β3a N terminus, the construct exhibits slow tail currents. The amplitude of the residual slow tail currents was used as an assay of the time course of trypsin digestion. (F) The trypsin-mediated change in tail current amplitude of the mβ3a-β2(6Q) construct is indistinguishable from removal of inactivation mediated by the wild-type mβ3a N terminus. (G) Traces show trypsin-mediated removal of inactivation for an N terminus consisting of the first 20 residues of β3a, followed by 10 glutamine residues then appended to TM1 of the β2 subunit (β3a(1–20)-10Q-β2). (H) The time course of trypsin-mediated removal of inactivation is plotted for both β3a(1–20)-10Q-β2 and β3a(1–20)-20Q-β2, with both being indistinguishable from wild-type mβ3a.